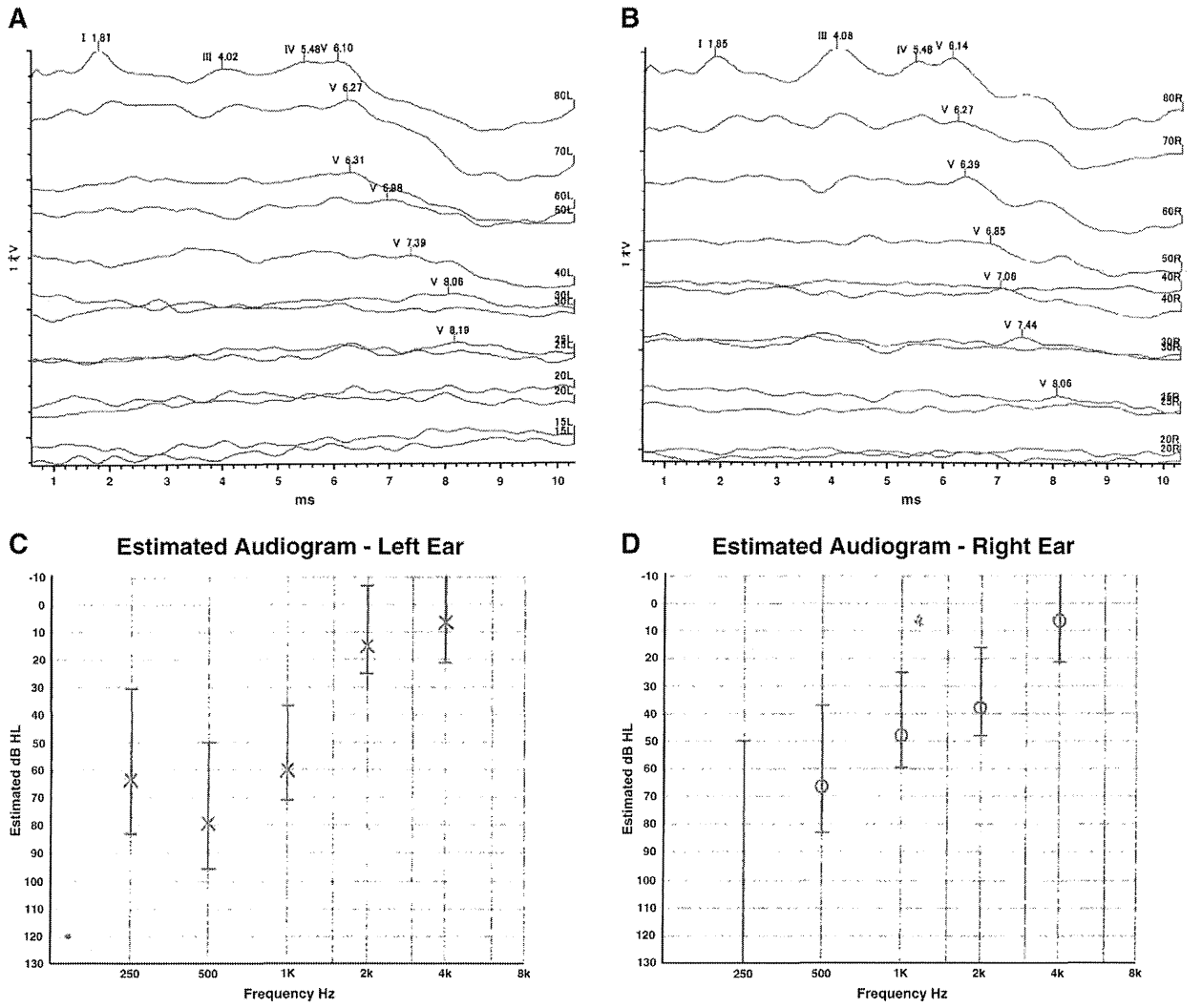

Fig. 2. Auditory assessment of individual IV-3 (proband). Both sides of ABRs (A: left, B: right) showing well waveforms at wave V down to 40 dB. The estimated audiograms by ASSR (C: left, D: right) show reverse-slope hearing loss.

in an arginine-to-tryptophan substitution at codon 143 (R143W) and heterozygosity for R859P mutation of *WFS1*. Individual IV-1 had normal hearing and just heterozygosity for the R143W mutation of GSB2. Individual III-2 had normal hearing and no mutations of *GJB2* and *WFS1*. Individual III-5 was 34 years old, and had moderate sensorineural hearing impairment at all frequency levels (Fig. 3B). Sequencing of *GJB2* and *WFS1* revealed compound heterozygosity for the V37I and R143W mutation of *GJB2* and heterozygosity for R859P mutation of *WFS1*. Individual II-5 was 61 years old, and had moderate hearing loss gently sloping (Fig. 3C). Sequencing of *GJB2* and *WFS1* revealed homozygosity for the V37I mutation of GJB2, but not *WFS1* mutations. Individual II-11 had normal hearing and heterozygosity for the R143W mutation of GJB2.

4. Discussion

We found a family who has both a *GJB2* mutation and a *WFS1* mutation. The individuals who have heterozygosity of *GJB2* mutations and heterozygosity of *WFS1* mutations show low-frequency hearing loss. On the other hand, flat loss configuration was found in the individual who has compound heterozygosity of *GJB2* mutation and *WFS1* mutation, and gradual high tone loss was seen in the individual who has homozygosity of *GJB2* mutation without *WFS1* mutations. According to our results, the individual who has both *GJB2* and *WFS1* mutations shows the *GJB2* phenotype. We should think about the effect of age modifying the hearing phenotype. However, the hearing impairments of III-5, 34 years old woman, andII-5, 61 years old man, are much worse at all frequencies than ISO 7029 norms, which were applied to establish 95th percentile threshold values for presbyacusis at each frequency in relation to the patient's age and sex (ISO 7029–2000 [ISO, 2000]).

Both V37I and R143W mutations in *GJB2* are non-inactivating mutations (Snoeckx et al., 2005). It has been reported that non-inactivating mutations of *GJB2* show less severe hearing impairment than inactivating mutations (Angeli, 2008; Cryns et al., 2004). As in this report, both homozygosity of V37I mutation and compound heterozygosity of V37I and R143W mutations show moderate hearing impairment, even if they are comorbid with *WFS1* mutation.

Both parents of subject III-5 had no *WFS1* mutations, indicating that heterozygosity for R859P mutation of *WFS1* of individual III-5 is a new mutation. R859P mutation of *WFS1*has been previously reported in one large family from the United States (Gurtler et al., 2005). A missense mutation at c.2576G>C results in an amino acid substitution, p.R859P, in a highly conserved area across human, mouse, and

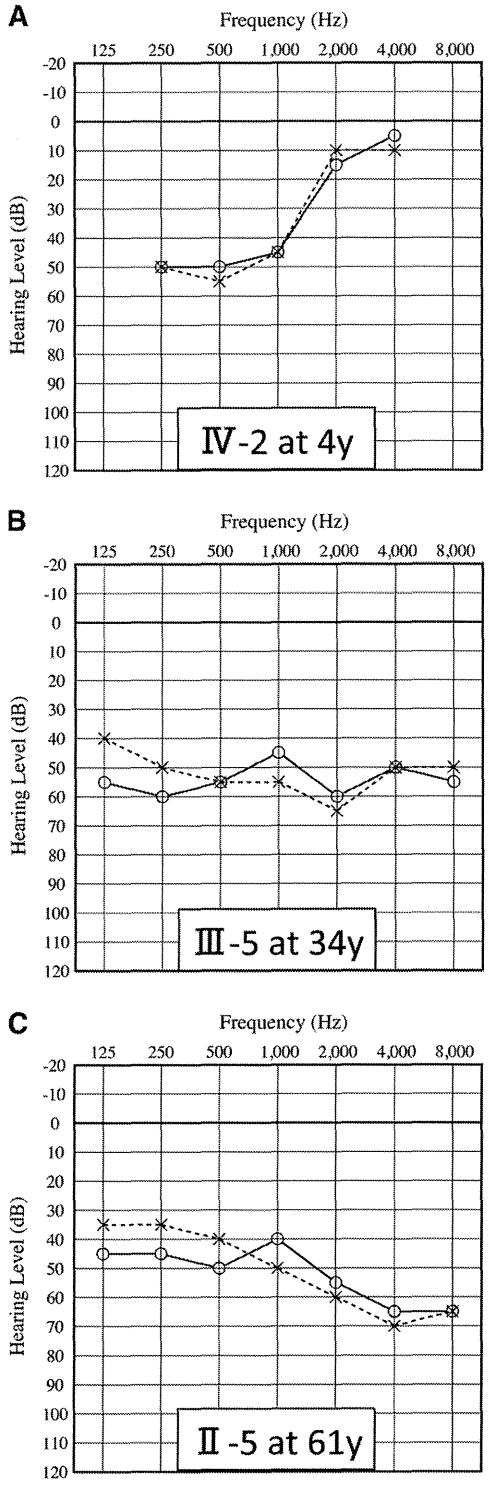

Fig. 3. Representative audiograms of individual IV-2 (A), individual III-5 (B), and individual II-5 (C) showing pure-tone audiometry results for air conduction bilaterally. Circles, air conduction right ear; crosses, air conduction left ear. Severe reverse-slope loss is seen in IV-2, whereas moderate flat hearing loss in III-5 and moderate hearing loss with mild ski-slope type inII-5.

rat. The mutation substitutes proline for naturally occurring arginine; this substitution is known to disrupt helical chains. It is likely that the mutation significantly alters the secondary structure of wolframin by creating a bending point in the amino acid chain in the C-terminal domain. The wolframin function in the cochlea is unknown so far, but if wolframin and connexin 26 serve very different functions in the cochlea, the person who has comorbid *WFS1* and GSB2 mutations would show additive hearing impairment. However, the comorbid case showed non-additive hearing loss, which indicates that wolframin may play a relevant role with connexin 26. That is to say, it is possible that wolframin in the cochlea works in potassium recycling. It is reported that sodium–potassium ATPase b1 subunit is a molecular partner of wolframin (Zatyka et al., 2008), which may support our hypothesis. However, genotype and phenotype correlation may not be such a simple process, but there may be many genetic and environmental factors. The duality of *WFS1* in frequency-specific hearing, which is the observation that recessive inactivating mutations cause high-frequency hearing loss as part of Wolfram syndrome and dominant noninactivating missense mutations cause low-frequency hearing loss, is still mysterious.

In conclusion, we have reported on a family which has comorbid mutations of *GJB2* and *WFS1* mutations, including one individual who has both *GJB2* and *WFS1* mutations and shows a *GJB2* phenotype. We should think about the possibility of comorbid gene mutation for hearing impairment. It is worth noting that more than 2 genetic mutations responsible for deafness can occur in one individual, and that the hearing characteristics of phenotype help us to speculate on molecular functions in the cochlea.

Acknowledgments

This work was supported by JSPS KAKENHI 22791627 and a Grant-in-Aid for Clinical Research from the National Hospital Organization.

References

Angeli, S.I., 2008. Phenotype/genotype correlations in a DFNB1 cohort with ethnical diversity. Laryngoscope 118, 2014–2023.
Bespalova, I.N., et al., 2001. Mutations in the Wolfram syndrome 1 gene (WFS1) are a common cause of low frequency sensorineural hearing loss. Hum. Mol. Genet. 10, 2501–2508.
Bom, S.J., Van Camp, G., Cryns, K., Admiraal, R.J., Huygen, P.L., Cremers, C.W., 2002. Autosomal dominant low-frequency hearing impairment (DFNA6/14): a clinical and genetic family study. Otol. Neurotol. 23, 876–884.
Brodwolf, S., Boddeker, I.R., Ziegler, A., Rausch, P., Kunz, J., 2001. Further evidence for linkage of low-mid frequency hearing impairment to the candidate region on chromosome 4p16.3. Clin. Genet. 60, 155–160.
Cryns, K., et al., 2003a. Mutational spectrum of the WFS1 gene in Wolfram syndrome, nonsyndromic hearing impairment, diabetes mellitus, and psychiatric disease. Hum. Mutat. 22, 275–287.
Cryns, K., et al., 2003b. The WFS1 gene, responsible for low frequency sensorineural hearing loss and Wolfram syndrome, is expressed in a variety of inner ear cells. Histochem. Cell Biol. 119, 247–256.
Cryns, K., et al., 2004. A genotype—phenotype correlation for GJB2 (connexin 26) deafness. J. Med. Genet. 41, 147–154.
Dai, P., et al., 2009. GJB2 mutation spectrum in 2,063 Chinese patients with nonsyndromic hearing impairment. J. Transl. Med. 7, 26.
Estivill, X., et al., 1998. Connexin-26 mutations in sporadic and inherited sensorineural deafness. Lancet 351, 394–398.
Gurtler, N., et al., 2005. Two families with nonsyndromic low-frequency hearing loss harbor novel mutations in Wolfram syndrome gene 1. J. Mol. Med. 83, 553–560.
Higashi, K., 1991. Otologic findings of DIDMOAD syndrome. Am. J. Otol. 12, 57–60.
Inoue, H., et al., 1998. A gene encoding a transmembrane protein is mutated in patients with diabetes mellitus and optic atrophy (Wolfram syndrome). Nat. Genet. 20, 143–148.
ISO (International Organization for Standardization), 2000. ISO 7029-2000: Acoustics—Statistical Distribution of Hearing Thresholds as a Function of Age, 2nd ed. International Organization for Standardization, Geneva.
Kunst, H., Marres, H., Huygen, P., Van Camp, G., Joosten, F., Cremers, C., 1999. Autosomal dominant non-syndromal low-frequency sensorineural hearing impairment linked to chromosome 4p16 (DFNA14): statistical analysis of hearing threshold in relation to age and evaluation of vestibulo-ocular functions. Audiology 38, 165–173.
Lesperance, M.M., Hall III, J.W., San Agustin, T.B., Leal, S.M., 2003. Mutations in the Wolfram syndrome type 1 gene (WFS1) define a clinical entity of dominant

low-frequency sensorineural hearing loss. Arch. Otolaryngol. Head Neck Surg. 129, 411–420.
Maeda, S., et al., 2009. Structure of the connexin 26 gap junction channel at 3.5 A resolution SUPPLEMENTARY INFORMATION. Nature 458, 597–602.
Matsunaga, T., 2009. Value of genetic testing in the otological approach for sensorineural hearing loss. Keio J. Med. 58, 216–222.
Matsunaga, T., Hirota, E., Bito, S., Niimi, S., Usami, S., 2006. Clinical course of hearing and language development in GJB2 and non-GJB2 deafness following habilitation with hearing aids. Audiol. Neurootol. 11, 59–68.
Morell, R.J., et al., 1998. Mutations in the connexin 26 gene (GJB2) among Ashkenazi Jews with nonsyndromic recessive deafness. N. Engl. J. Med. 339, 1500–1505.
Ohtsuka, A., et al., 2003. GJB2 deafness gene shows a specific spectrum of mutations in Japan, including a frequent founder mutation. Hum. Genet. 112, 329–333.
Pennings, R.J., et al., 2003. Progression of low-frequency sensorineural hearing loss (DFNA6/14-WFS1). Arch. Otolaryngol. Head Neck Surg. 129, 421–426.
Smith, R.J., Bale Jr., J.F., White, K.R., 2005. Sensorineural hearing loss in children. Lancet 365, 879–890.
Snoeckx, R.L., et al., 2005. GJB2 mutations and degree of hearing loss: a multicenter study. Am. J. Hum. Genet. 77, 945–957.
Strom, T.M., et al., 1998. Diabetes insipidus, diabetes mellitus, optic atrophy and deafness (DIDMOAD) caused by mutations in a novel gene (wolframin) coding for a predicted transmembrane protein. Hum. Mol. Genet. 7, 2021–2028.
Young, T.L., et al., 2001. Non-syndromic progressive hearing loss DFNA38 is caused by heterozygous missense mutation in the Wolfram syndrome gene WFS1. Hum. Mol. Genet. 10, 2509–2514.
Zatyka, M., et al., 2008. Sodium–potassium ATPase 1 subunit is a molecular partner of wolframin, an endoplasmic reticulum protein involved in ER stress. Hum. Mol. Genet. 17, 190–200.
Zdebik, A.A., Wangemann, P., Jentsch, T.J., 2009. Potassium ion movement in the inner ear: insights from genetic disease and mouse models. Physiology (Bethesda) 24, 307–316.

Functional Interaction Between Mesenchymal Stem Cells and Spiral Ligament Fibrocytes

Guang-wei Sun,[1]* Masato Fujii,[2] and Tatsuo Matsunaga[1]*

[1]The Laboratory of Auditory Disorders, National Institute of Sensory Organs, National Tokyo Medical Center, Tokyo, Japan
[2]Division of Hearing and Balance Research, National Institute of Sensory Organs, National Tokyo Medical Center, Tokyo, Japan

Spiral ligament fibrocytes (SLFs) play an important role in normal hearing as well as in several types of sensorineural hearing loss attributable to inner ear homeostasis disorders. Our previous study showed that transplantation of mesenchymal stem cells (MSCs) into the inner ear of rats with damaged SLFs significantly accelerates hearing recovery compared with rats without MSC transplantation. To elucidate this mechanism of SLF repair and to determine the contribution of transplanted MSCs in this model, we investigated the mutual effects on differentiation and proliferation between MSCs and SLFs in a coculture system. Factors secreted by SLFs had the ability to promote the transdifferentiation of MSCs into SLF-like cells, and the factors secreted by MSCs had a stimulatory effect on the proliferation of SLFs. Cytokine antibody array analysis revealed the involvement of transforming growth factor-β (TGF-β) in SLF proliferation induced by MSCs. In addition, a TGF-β inhibitor reduced SLF proliferation induced by MSC stimulation. Our results suggest that there are two mechanisms of hearing recovery following transplantation of MSCs into the inner ear: 1) MSCs transdifferentiate into SLF-like cells that compensate for lost SLFs, and 2) transplanted MSCs stimulate the regeneration of host SLFs. Both mechanisms contribute to the functional recovery of the damaged SLF network.

Key words: mesenchymal stem cells; spiral ligament fibrocytes; transplantation

Mammalian cochlear fibrocytes of the mesenchymal nonsensory regions play an important role in the cochlear physiology of hearing, including the transport of potassium ions to generate an endocochlear potential in the endolymph that is essential for the transduction of sound by hair cells (Weber et al., 2001; Wangemann, 2002; Delprat et al., 2005). Recent studies have also highlighted the importance of these fibrocytes in the spiral ligament (SL) in the pathogenesis of sensorineural hearing loss. Several studies have indicated the involvement of SL degeneration in the mechanism of hearing loss that is due to aging (Hequembourg and Liberman, 2001; Spicer and Schulte, 2002), excessive noise (Hirose and Liberman, 2003), or genetic mutations (Minowa et al., 1999).

The spiral ligament fibrocytes (SLFs) are divided into types I–V based on their structural features, immunostaining patterns, and general location (Spicer and Schulte, 1996). In contrast to sensory cells, SLFs are able to repopulate themselves after noise or drug exposure in the mammalian inner ear (Roberson and Rubel, 1994; Hirose and Liberman, 2003; Lang et al., 2003). We previously developed a rat model of acute sensorineural hearing loss attributable to the dysfunction of SLFs induced by a mitochondrial toxin, 3-nitropropionic acid (3NP; Hoya et al., 2004; Okamoto et al., 2005; Kamiya et al., 2007; Mizutari et al., 2011). The main cause of hearing loss in this model is apoptosis of SLFs, without any changes in the organ of Corti. In addition, hearing recovery that occurs after 3NP exposure is accompanied by the regeneration of SLFs (Kamiya et al., 2007; Mizutari et al., 2011). The reconstruction of the potassium recycling route by SLF regeneration might lead to normalization of the endocochlear potential and hearing recovery.

After mesenchymal stem cells (MSCs) are transplanted into the inner ear of 3NP-treated rats, some of these stem cells are detected in the injured area of the SL, which correlates with a significantly greater hearing

Contract grant sponsor: Ministry of Education, Culture, Sports, Science and Technology of Japan; Contract grant number: 20591996 (to G.-w.S.); Contract grant sponsor: Ministry of Health, Labour, and Welfare of Japan; Contract grant number: H16-Kankakuki-006 (to T.M.).

*Correspondence to: Guang-wei Sun, The Laboratory of Biomedical Material Engineering, Dalian Institute of Chemical Physics, The Chinese Academy of Sciences, 457 Zhongshan R.d., Dalian 116023, China. E-mail: sunrise124@gmail.com. or Tatsuo Matsunaga, The Laboratory Auditory Disorders, National Institute of Sensory Organs, National Tokyo Medical Center, 2-5-1 Higashigaoka, Meguro, Tokyo 152-8902, Japan. E-mail: matsunagatatsuo@kankakuki.go.jp

Received 29 August 2011; Revised 3 March 2012; Accepted 20 March 2012

Published online in Wiley Online Library (wileyonlinelibrary.com). DOI: 10.1002/jnr.23067

recovery than occurs in control animals. The transplanted MSCs in the SL also express gap junction proteins between neighboring cells (Kamiya et al., 2007). The number of transplanted MSCs detected in the SL did, however, lead us to question whether those MSCs are sufficient for the supplementation of lost SLFs. To elucidate the mechanism of hearing recovery by MSC transplantation, we investigated the interaction between MSCs and SLFs as well as possible signaling mechanisms that may be involved in this interaction.

MATERIALS AND METHODS

Composition of Media and Growth Factors

Minimum essential medium (MEM) and RPMI 1640 supplemented with 9% fetal calf serum (FCS) were obtained from Invitrogen (Carlsbad, CA). Recombinant human transforming growth factor-β1 (TGF-β1) and TGF-β3 (R&D Systems, Minneapolis, MN) were used at a final concentration of 10 ng/ml. SB-431542 (Sigma-Aldrich, St. Louis, MO) and SU4984 (Calbiochem, Ober der Roth, Germany) were each added to cells at a concentration of 10 μM.

Antibodies

The antibodies used in this study are as follows: Na^+/K^+-ATPase α-1 and Na^+/K^+-ATPase β-1 (Santa Cruz Biotechnology, Santa Cruz, CA); Na-K-2Cl cotransporter (NKCC1; ARP, Belmont, MA); connexin 31 (Cx31; Zymed, Carlsbad, CA); vimentin and aquaporin 1 (Abcam, Cambridge, MA); S-100 (Sigma-Aldrich); CD16/32, CD45, CD44, mouse IgG2a isotype control, and mouse IgG2b isotype control (eBioscience, San Diego, CA); and CD29, CD49e, and streptavidin-fluorescein isothiocyanate (BD Pharmingen, San Diego, CA). The appropriate species-specific antibodies conjugated to either Alexa Fluor 488 or Alexa Fluor 568 (1:500; Molecular Probes, Eugene, OR) were used as secondary antibodies.

Cell Culture

Male C3H/HeJJcl mice (6 weeks old and postnatal day [P] 0) were used in the present study. All experiments were conducted in accordance with the guidelines of the National Institutes of Health and the Declaration of Helsinki. After anesthetization with xylazine (15 mg/kg, i.p.) and ketamine (80 mg/kg, i.p.), the mice were sacrificed. The inner ears were harvested rapidly, and the SLs from two ears were dissected at 4°C under aseptic conditions. The stria vascularis was carefully removed from the SLs using tweezers. The entire SL segment was collected and minced into small pieces with corneal scissors. The minced pieces were placed in type I collagen-coated Petri dishes (BD Pharmingen) in MEM supplemented with 9% FCS. The dish was kept in an incubator (37°C; 5% CO_2, 95% air) with maximum humidity, and the culture medium was changed every 3 days. Cells from passages 2–4 were stored with Cell Banker reagent (Juji Field, Tokyo, Japan) at −80°C.

We prepared MSCs as described by Islam et al. (2006). Briefly, to initiate the MSC cultures, bone marrow cells from C3H/HeJJcl mice were plated in tissue culture dishes and kept in a humidified incubator with 5% CO_2 at 37°C for 72 hr, at which point nonadherent cells were removed by changing the medium. The primary culture was then trypsinized and passaged to a new culture dish with a split ratio of 1:2. Subsequent passages were done when the culture approached confluence. Cells from passages 5–10 were used for the present investigation.

Culture medium from MSCs or SLFs was filtered with a 0.22-μm syringe filter (Millipore, Billerica, MA) to remove cells and was then used as conditioned medium. The conditioned medium was added to cells at a 1:1 (vol/vol) ratio with standard medium. For effects on cell cultures, MSCs and SLFs were plated on Petri dishes with standard medium for 3 days and then cultured with conditioned medium.

Flow Cytometry

Cells were incubated with antibodies for 30 min on ice and then centrifuged at 200*g* for 5 min. The antibody solution was removed, and cells were resuspended in ice-cold Hank's medium (Invitrogen) containing 2 μg/ml propidium iodide (Sigma-Aldrich) to distinguish between dead and living cells. The surface markers expressed on these cells were then analyzed by flow cytometry (Epics Altra with HyPerSort cell sorting system; Beckman Coulter, Fullerton, CA).

Immunocytochemical Staining

SLFs and MSCs placed on the Lab-Tek Chamber Slide System (Nunc, Rochester, NY) or in BD Falcon Cell Culture flasks (BD Pharmingen) were cultured with or without conditioned medium. Cultured cells were fixed in 4% paraformaldehyde (PFA). For the cells cultured in flasks, fixed cells were attached to slides with the cytospin method. Incubation with primary and secondary antibodies was carried out in phosphate-buffered saline (PBS) containing 1% normal goat serum (Sigma-Aldrich) overnight at 4°C or for 1 hr at room temperature. For negative controls, the primary antibody was omitted. Nuclear staining was performed with 4′6-diamidino-2-phenylindole dihydrochloride (DAPI; Sigma-Aldrich). The specimens were viewed with a laboratory microscope (DM 2500; Leica, Houston, TX).

Immunocytochemistry of Tissue Sections

Inner ears were isolated from male C3H/HeJJcl mice. Paraffin-embedded temporal bone blocks were sectioned horizontally at 5 μm. After deparaffinization, the sections were blocked with 10% normal goat serum (Sigma-Aldrich) diluted in 0.01 M PBS for 1 hr at room temperature. Incubation with primary and secondary antibodies was carried out in PBS containing 1% normal goat serum overnight at 4°C or for 1 hr at room temperature. For negative controls, the primary antibody was omitted. Nuclear staining was performed with DAPI. The appropriate species-specific antibodies conjugated to either Alexa Fluor 488 or Alexa Fluor 568 were used as secondary antibodies. The specimens were viewed with the DM 2500 microscope (Leica, Houston, TX).

DNA Arrays

The following cells were compared: 1) untreated MSCs (control) and MSCs cultured for 1 week with conditioned

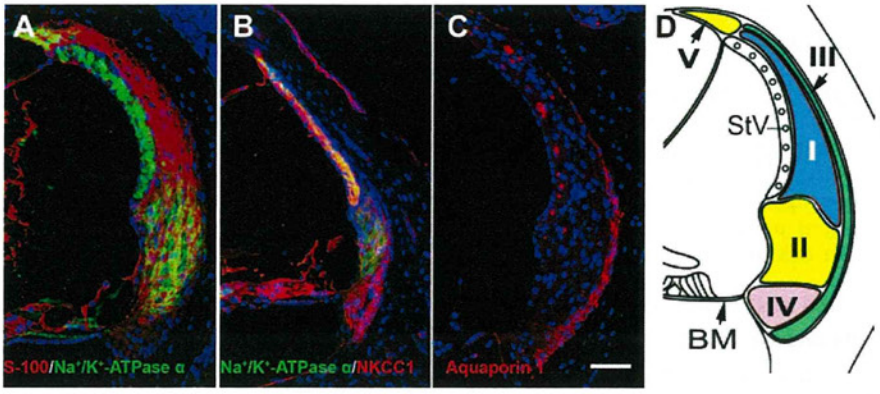

Fig. 1. Lateral wall from the middle turn of a C3H/HeJJcl mouse cochlea. **A–C:** Sections stained for S-100 (A), Na^+/K^+-ATPase α1 (A,B), NKCC1 (B), and aquaporin 1 (C) are shown. Type I fibrocytes of the SL were positive for S-100. Type II and type V fibrocytes also stained with antibodies to S-100, Na^+/K^+-ATPase α1, and NKCC1; however, they were distinguishable from type IV fibrocytes by their positive staining for S-100 and Na^+/K^+-ATPase α1. Type III fibrocytes were positive for aquaporin 1 (C). **D:** Illustration of the lateral wall region shown in A–C, with the fibrocyte populations indicated. BM, basilar membrane; StV, stria vascularis. Scale bar = 50 μm.

medium from SLFs and 2) untreated SLFs (control) and SLFs cultured for 1 week with conditioned medium from MSCs (n = 1). Isolation of RNA, hybridization, and cDNA array analyses were performed by Filgen (Agilent Technologies Inc., Tokyo, Japan) using OpArray mouse v4.0 (Filgen). The Microarray Data Analysis Tool, version 1.5 (Filgen), was used to quantify signal intensities. As per the manufacturer's instructions (Filgen), changes in mRNA expression were considered meaningful if there was a greater than twofold change relative to the control values. Data were analyzed using Microarray Data Analysis Tool, version 3.2 (Filgen).

Cytokine Antibody Arrays

When MSCs were nearly confluent, they were cultured in RPMI 1640 with 0.2% FCS for 24 hr. The medium was harvested and filtered with a 0.22-μm syringe filter to remove cell debris (n = 1). Cytokine antibody array analyses were performed by Filgen using a RayBio biotin label-based mouse cytokine antibody array (L-308; RayBiotech, Norcross, GA). The quantified secretion of each cytokine was compared as a ratio using Microarray Data Analysis Tool, version 1.5. Changes in cytokine secretion were considered meaningful if there was a greater than twofold change relative to the control values.

Statistical Analysis

All statistical analyses were performed using a one-way analysis of variance. OriginPro 7.5 (OriginLab, Northampton, MA) was used for comparisons between experimental groups and control groups. $P < 0.01$ was considered significant.

RESULTS

Histological Observations

The staining pattern of cells that make up the cochlea from a 6-week-old C3H/HeJJcl mouse is shown in Figure 1. Type I SLFs, which are found lateral to the stria vascularis (Takahashi and Kimura, 1970), showed positive immunological staining for S-100 (Fig. 1A). These fibrocytes did not show staining for Na^+/K^+-ATPase α1 (Fig. 1A,B) or NKCC1 (Fig. 1B). Type II fibrocytes, which are located lateral to the spiral prominence (Takahashi and Kimura, 1970), and type V fibrocytes, which are equivalent to the type II fibrocytes in the suprastrial region (Spicer and Schulte, 1996), were positive for Na^+/K^+-ATPase α1 (Fig. 1A,B) and NKCC1 (Fig. 1B) staining. Type II and type V fibrocytes were also positive for S-100 staining (Fig. 1A). Aquaporin 1 staining was detected on type III fibrocytes only (Fig. 1C), which are found adjacent to the bone in the inferior region of the SL (Spicer and Schulte, 1991). Type IV fibrocytes, which are located inferior to the basilar membrane (Spicer and Schulte, 1991), were distinguishable from type II fibrocytes because they were positive for NKCC1 and negative for Na^+/K^+-ATPase α1 and S-100 staining in these mice (Fig. 1A,B). The immunohistochemical profile of SLFs is shown in Table I. Each type of SLF could be distinguished based on its pattern of antibody staining.

TABLE I. Immunohistochemical Profile of SLF Types in C3H/HeJJcl Mice

Antigen	Type I	Type II/V	Type III	Type IV
S-100	+	+	−	−
Na^+/K^+-ATPase α1	−	+	−	−
NKCC1	−	+	−	+
Aquaporin 1	−	−	+	−

Observations of the Growth and Differentiation of Cultured SLFs

The first signs of growth in the SL explants were observed within 24–48 hr. Cell expansion was observed

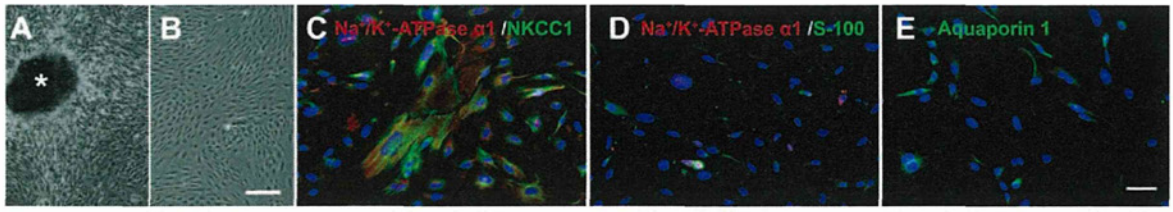

Fig. 2. Pure cultures of postnatal mice SLFs were obtained and stably maintained in vitro. **A:** Primary culture of SLFs after 21 days in culture. Spindle-shaped cells extending from the edges of the explant (asterisk) were observed. **B:** Cells that had been passaged one time with homogenous morphology. The expression of each type-specific set of SLF markers was detected in cultured SLFs. **C–E:** Na^+/K^+-ATPase α1 (type II), NKCC1 (type II and IV), S-100 (type I and II), aquaporin 1 (type III). Scale bars = 50 μm in A (applies to A,B); 50 μm in E (applies to C–E).

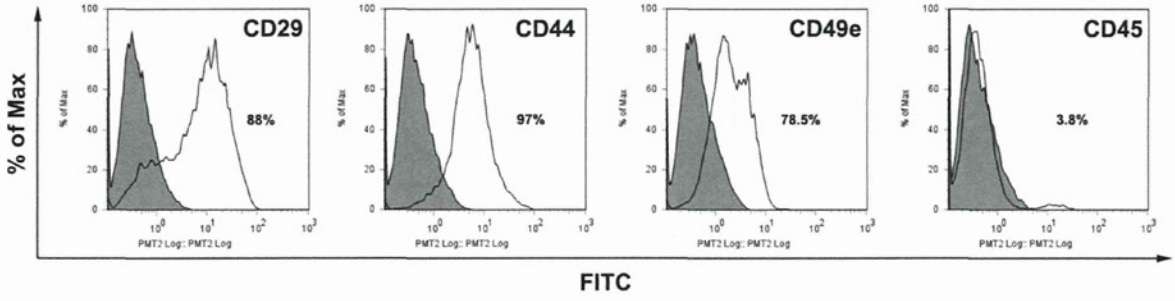

Fig. 3. Characterization of MSCs. MSCs at passages 5 and 10 were positive for CD29, CD44, and CD49e staining and were negative for CD45 staining. Open areas show the percentages of positive cells; shaded areas show cells treated with isotope antibodies.

initially as spindle-shaped cells extending from the edges of the explants (Fig. 2A). The primary culture was subcultured at 21 days. Spindle-shaped cells having large nuclei and cytoplasmic regions with slender, irregular processes were observed (Fig. 2B). The morphological characteristics of the subculture were consistent with previous studies (Gratton et al., 1996; Suko et al., 2000). The number of SLFs significantly increased in the adherent culture (by ~ 376-fold after 21 days in culture; see Fig. 4F). Type I SLFs were positive for S-100 staining but negative for Na^+/K^+-ATPase α1 and NKCC1 staining. Type II SLFs were positive for Na^+/K^+-ATPase α1, NKCC1, and S-100 staining. Type III SLFs were positive for aquaporin 1 staining only, whereas type IV SLFs were positive for NKCC1 staining (Fig. 2C–E, Table I). These results suggested that this culture system included all types of SLFs. Most of the cells in this culture system were type II (34.06%) and type IV (62.64%) fibrocytes. The percentages of type I and type III fibrocytes were 2.2% and 13.2%, respectively.

Characterization of MSCs

MSC cells from passages 5 and 10 were used for investigation of cell surface markers. Flow cytometry analysis indicated that these MSCs were positive for CD29, CD44, and CD49e staining but were negative for CD45 staining (Fig. 3) before transplantation, which is similar to previously isolated murine MSCs (Islam et al., 2006).

Effects of MSC Culture Supernatants on SLFs

Next, the effect of molecules secreted by MSCs on SLFs was investigated. The addition of culture supernatants from MSCs markedly stimulated the proliferation of SLFs (twofold) after 21 days in vitro (Fig. 4F). To ascertain whether the cellular characteristics were affected by the molecules secreted by MSCs, we checked the expression of SLF markers on those cells. Previous studies have indicated that the fibrocyte populations that are most likely to show degeneration in the damaged cochlea are the type II and IV fibrocytes (Kamiya et al., 2007). Thus we focused here on investigating the expression of type II and IV markers. Immunostaining showed that the expression of SLF type markers decreased, whereas the percentage of vimentin-positive cells increased, in SLFs cultured with MSC conditioned medium compared with the expression in SLFs cultured without the conditioned medium (Fig. 4A,B,E). Vimentin is a marker of mesenchymal cells and is detected in the mesenchyme-derived tissue of the inner ear (Kuijpers et al., 1992). Increases in vimentin synthesis are associated with rapidly growing cells (Benzeev, 1985). In our study, vimentin immunoreactivity was observed in almost all SLFs in P0 C3H/HeJJcl mice (Fig. 4C), whereas no NKCC1 was detected (data

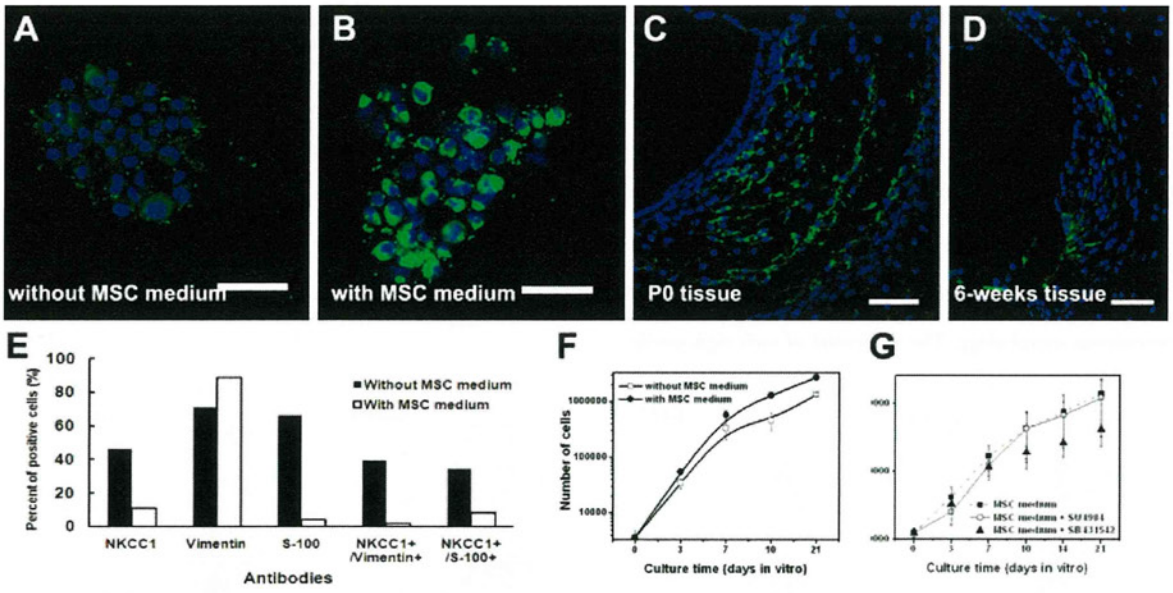

Fig. 4. Characteristics of SLFs cultured with or without culture supernatants from MSCs for 21 days. Vimentin expression increased in SLFs in culture in the presence of MSC conditioned medium (**B**) but not in its absence (**A**). **C:** In P0 C3H/HeJJcl mice, strong vimentin immunoreactivity was observed in fibrocytes of the SL. **D:** At 6 weeks after birth, vimentin expression was restricted to a subgroup of the SLFs. **E:** Expression of vimentin in SLFs in the absence or presence of MSC conditioned medium. **F:** Growth curves of SLF cells cultured with or without MSC conditioned medium. **G:** SLF proliferation stimulated by MSC conditioned medium was inhibited by the addition of SB-431542 and SU4984. The percentage of the cells in each bar chart indicates the mean ± SD of three independent experiments. Nuclei were stained with DAPI (blue). Scale bars = 50 μm.

not shown). At 6 weeks after birth, vimentin expression was restricted to a subpopulation of SLFs (Fig. 4D). Our results suggest that factors in the supernatants of MSCs grown in culture have the ability to stimulate the proliferation of SLFs and that a high proportion of these proliferating SLFs has marker expression features that are similar to those of SLFs early in postnatal development.

Effects of SLF Culture Supernatants on MSCs

To investigate whether SLF conditioned medium has effects on the proliferation and differentiation of MSCs, MSCs were cultured with or without conditioned medium. In the initial cultures, no MSCs were positive for Na^+/K^+-ATPase β1 (Fig. 5A) or NKCC1 (data not shown) expression, both of which are type II and IV SLF marker proteins (Schulte and Steel, 1994). After the culture, although MSC-derived cells expressed Na^+/K^+-ATPase β1 spontaneously, the addition of SLF conditioned medium increased the expression of Na^+/K^+-ATPase β1 (Fig. 5B) compared with MSC cultures without the conditioned medium (Fig. 5E; $P < 0.05$). Some MSC-derived cells were also positive for NKCC1 expression (Fig. 5C). No cells that were positive for S-100 expression were detected in the initial MSC cultures (data not shown). With culture on collagen-coated dishes at a low density, S-100-positive cells were, however, detected (data not shown). The proportion of S-100-positive cells was not affected by the addition of SLF conditioned medium (Fig. 5D; 62.4% vs. 69.72%, 14 days in vitro).

We also examined the effects of conditioned medium from SLFs on MSC proliferation. The total number of cells obtained after the addition of SLF conditioned medium was similar to that obtained with standard medium (Fig. 5F; $P = 0.718$). Our results suggest that the factors secreted by SLFs promote MSC transdifferentiation into SLF-like cells but do not affect MSC proliferation.

Cell Microarray Analysis and Cell Proliferation Assay

To investigate the underlying cellular and molecular differences between the cells cultured in standard medium and those cultured with conditioned medium, we performed a gene expression analysis on both MSCs and SLFs using the OpArray mouse v4.0 array. Significant changes in gene expression were filtered according to the background expression of individual genes and at least a twofold difference in expression between the samples and controls. Detailed examination of the biological functions of differentially expressed genes between MSCs with or without SLF conditioned medium revealed genes related to stem cell development, the

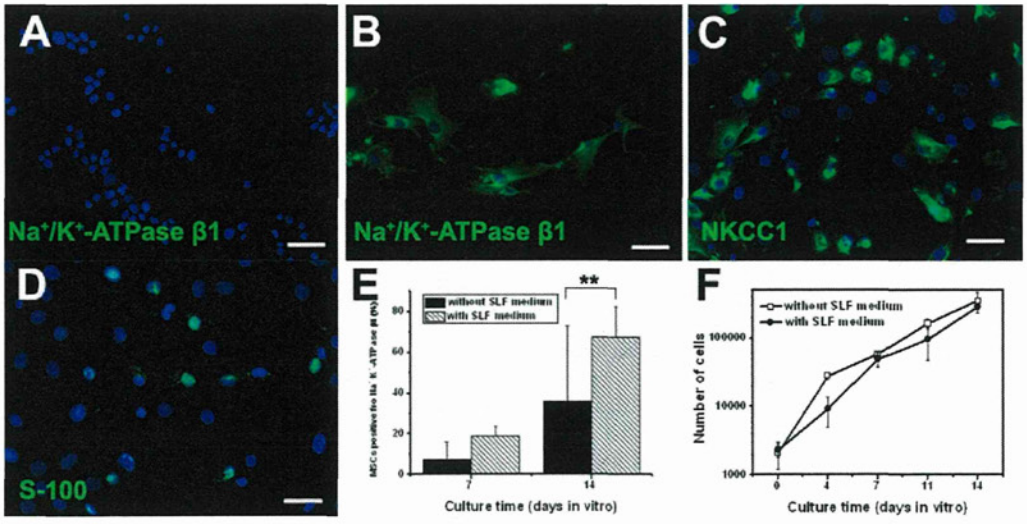

Fig. 5. Characteristics of MSCs cultured with or without culture supernatants from SLFs. **A:** SLF-like cell differentiation of MSCs. No cells that were positive for Na^+/K^+-ATPase β1 expression were found in the initial MSC cultures. **B,E:** When MSCs were plated on collagen-coated dishes, the addition of SLF conditioned medium (with SLF) increased the expression of Na^+/K^+-ATPase β1 (B,E) compared with cultures without conditioned medium (E; $^{**}P < 0.05$). **C,D:** Furthermore, cells that were positive for the expression of NKCC1 (C) and S-100 (D) were detected in MSCs cultured with SLF conditioned medium. **F:** Conversely, culture supernatants from SLFs had no effect on promoting the proliferations of MSCs. The percentage of the cells in each bar chart indicates the mean ± SD of three independent experiments. Nuclei were stained with DAPI (blue). Scale bars = 50 μm.

TABLE II. Genes Differentially Expressed Between MSCs Cultured With and Without SLF Conditioned Medium

Category	Increased by more than twofold	Decreased by more than twofold
Stem cell development	*Tfrc, Tnfrsf12a, Ednrb, Nrcam, Hells, Grem1, Slc2a1, Ccna2, S100a4, Angpt1, Mmp14*	*Wif1, Ascl1, Ibsp, Myod1, Col4a6, Thbs1, Prok2, Mmp13, phex, Mtss1*
Wnt pathway	*Pitx2, Wnt8a*	*Wif1*
Cell cycle	*Nek2, Ccna2, Mcm3*	*Trp63*
Apoptosis	*Hmox1, Tnfrsf12a, Hells, Lhx4*	*Myod1, Trp63, Gadd45b, Thbs1, Prok2, Dffb*

TABLE III. Genes Differentially Expressed Between SLFs Cultured With and Without MSC Conditioned Medium

Category	Increased by more than twofold	Decreased by more than twofold
Extracellular matrix and adhesion molecules	*Spp1, Tgfbi*	*Mmp11, Thbs1*
Wnt pathway		*Wisp2*
Notch pathway	*Dtx3, Gli2*	
TGF-β, BMP pathway	*Tgfbi*	
Apoptosis	*Pttg1, Lhx4, Atf5, Cyp2c38*	*Thbs1*
Growth factors	*Spp1*	
Cytokine and inflammatory responses	*Spp1, Atf5, tgfbi, Ifit1*	

Wnt pathway, the cell cycle, and apoptosis (Table II). In contrast, between SLFs cultured with or without MSC conditioned medium, genes involved in extracellular matrix and adhesion molecules, apoptosis, and cytokine and inflammatory responses as well as key determinants of cell fate (Wnt pathway, Notch pathway, and TGF-β pathway) were significantly different (Table III).

Furthermore, by using an array that focuses on mouse cytokines, we investigated factors secreted by MSCs. Ten factors were increased more than twofold in MSC conditioned medium compared with the medium in which no cells were cultured. The biological functions of those cytokines are related to apoptosis, the inflammatory response, and cell proliferation (data not shown). One of the secreted cytokines was TGF-β3, which is involved in cell proliferation (Huang and Huang, 2005). To determine the TGF-β responsible for regulating SLF proliferation, SB-431542, a specific inhibitor of the TGF-β type I receptor (TbRI; Laping et al., 2002), was added to MSC conditioned medium. SB-431542 partially inhibited SLF proliferation that was induced by MSC conditioned medium (Fig. 4G).

FGF2, which is also secreted by MSCs (Dormady et al., 2001; Sensebe et al., 1997), was not included in the cytokine array that we used in this study. Because FGF2 and its receptor, FGF-receptor 1 (FGFR1), are expressed at high levels in the lateral wall of postnatal mouse (Pickles, 2001), we also added the FGFR1 inhibitor SU4984 (Mohammadi et al., 1997) to MSC conditioned medium. This inhibitor did not, however, have

an effect on SLF proliferation in the presence of MSC conditioned medium (Fig. 4G).

DISCUSSION

Inner ear cell culture has been successfully reported in epithelial (Rarey and Patterson, 1989; Achouche et al., 1991; Melichar and Gitter, 1992) and endothelial (Bowman et al., 1985) cells. Recently, cell culture of SLFs has also been established and characterized for type I SLFs in gerbils (Gratton et al., 1996), mice (Suko et al., 2000), and rats (Yian et al., 2006). To date, however, there are no reports on the successful establishment of a concurrent culture of all types of SLFs, which more closely mimics the in vivo condition. In the present study, we attempted to establish such an SLF culture system using isolated cells from mice. Our cultured cells contained spindle-shaped cells, which are morphologically compatible with fibrocytes, and immunocytochemical analysis detected the markers of all four types of SLFs. This novel SLF culture system, which more closely mimics conditions in vivo, may be especially useful in elucidating the effects of a specific condition on the cochlear ion homeostasis.

Many factors are known to affect the differentiation of MSCs. These include soluble growth factors and cytokines (Otto and Lane, 2005; Bowers and Lane, 2007), mechanical stimuli (Lee et al., 2007), surface properties (Guo et al., 2008), and culture conditions (Song et al., 2007). Cell density has been reported to affect cell functions such as proliferation and differentiation (Bitar et al., 2008; Neuhuber et al., 2008). McBeath et al. (2004) have reported that human MSCs plated at lower density are more likely to become osteoblasts, whereas cells plated at higher density are more likely to become adipocytes. In the present study, MSCs did not express markers for SLFs under routine culture conditions. When MSCs were plated on collagen-coated dishes at a lower density, however, a small subgroup of MSCs differentiated into SLF-like cells spontaneously. The collagen coating was likely to have affected MSC differentiation into SLF-like cells, because the SL is made up of fibrocytes embedded in collagen fibrils (Tsuprun and Santi, 1999). Our results also showed that factors secreted by SLFs had the ability to promote MSCs to differentiate into SLF-like cells with no effects on their proliferation. In stem cells or progenitor cells, inhibition of proliferation induces differentiation (Hirose et al., 2006; Jung et al., 2008). Therefore, the lower proliferation of MSCs cultured with SLF conditioned medium may also explain the increase in MSC differentiation into SLF-like cells. The DNA array results showed several genes that were highly expressed in MSCs cultured with SLF conditioned medium. One of these factors, *Wnt8a*, is expressed in rhombomere 4 in embryonic day (E8) mouse (Bouillet et al., 1996) and is the canonical WNT that activates the WNT-β-catenin pathway (Katoh, 2005). *Wnt8* is expressed in the developing hindbrain in chick, mouse, and zebrafish, in which it has been implicated in stabilizing otic fate following induction (Ohyama et al., 2006; Freter et al., 2008). Studies have suggested that canonical Wnt signaling affects MSC proliferation and differentiation (Cho et al., 2000; Boland et al., 2004; De Boer et al., 2004). Further studies are needed to clarify the mechanism by which canonical Wnt signaling regulates MSC proliferation.

Our study clearly demonstrates that conditioned medium from MSCs stimulated SLF proliferation. The cells that were incubated with MSC conditioned medium showed increased expression of vimentin, which is a mesenchymal progenitor marker protein (Rose et al., 2008), whereas the expression of markers of mature SLFs decreased. Immunostaining data from tissue sections of mouse cochlea showed that vimentin was present in SLFs at P0 and that the intensity of labeling decreased after birth. Vimentin is associated with the mitotic apparatus and is related to the induction of cellular DNA synthesis and mitosis. It is involved in the extensive remodeling of cytoskeletal components that is required for mitosis, cell migration, and process outgrowth (Baserga, 1985; Ferrari et al., 1986), so increases in vimentin synthesis are associated with rapidly growing cells. In our study, vimentin immunoreactivity decreased during postnatal development of the SL (Fig. 4C,D). This decreased expression of vimentin in the SL could be indicative of declining mitotic activity across the whole SL, as has been observed in the mouse (Ruben, 1967; Mutai et al., 2009). At P0, vimentin-positive cells did not express markers of mature SLFs, which leads us to speculate that those cells were in an immature state. In the SL of 6-week-old mice, vimentin expression was restricted to a subpopulation of SLFs. SLFs are able to repopulate themselves after noise or drug exposure in the adult mammalian inner ear (Roberson and Rubel, 1994; Hirose and Liberman, 2003; Lang et al., 2003). Immature SLFs or stem cells that reside in the mature SL might explain how SLFs repair or replace themselves. Increased expression of vimentin along with the decreased expression of mature SLF markers that was observed in SLFs cultured with MSC conditioned medium might also be explained by the proliferation of immature SLFs that were stimulated by the factors secreted by the MSCs. Transplanted MSCs might induce the proliferation of such immature SLFs and may thus contribute to the repair of the damaged SL. Whether the stimulated vimentin-positive cells have the ability to differentiate into mature SLFs to restore the damaged SLF network must be clarified in further experiments.

Analyses using DNA and cytokine arrays revealed the involvement of TGF-β signaling in the effect of MSCs on SLFs. TGF-β stimulates or inhibits the growth and differentiation of cells (McCartney-Francis et al., 1998). Reciprocal interactions between the developing otic epithelium and the periotic mesenchymal tissue are critical for normal inner ear morphogenesis. As a secreted protein, TGF-β participates in these interactions in a variety of developing tissues (Massague, 1990; Kingsley, 1994). TGF-β3 is expressed throughout the cochlear epithelium at E13.5–E17.5 (Pelton et al., 1991).

The type II TGF-β receptor (TbRII), which mediates many of the biological responses to TGF-β, is found in the mesenchyme surrounding the inner ear (Wang et al., 1995). TGF-β ligands bind to heteromeric complexes of TbRI and TbRII (Massague, 1998; Shi and Massague, 2003). SB-431542, an inhibitor of TbRI (Laping et al., 2002), blocks the TGF-β-mediated proliferation of a mesenchymal cell line (Matsuyama et al., 2003). In this study, SB-431542 partially inhibited SLF proliferation that was induced by the addition of MSC conditioned medium, suggesting that TGF-β secreted from MSCs contributes to the proliferation of SLFs. Because the transplantation of stem cells, combined with specific growth factors and cytokines, has been thought to have great potential in regenerative medicine, the identification of paracrine factors from MSCs should be helpful in improving the success of MSC transplantation.

The DNA array results in SLFs stimulated with MSC conditioned medium revealed genes with a known role in apoptosis (Table III). Overexpression of the gene encoding *PTTG1*, one of these upregulated genes, decreases UV-induced apoptosis (Lai et al., 2007), and increased expression of *PTTG1* increases cell proliferation (Kakar and Jennes, 1999; Zhang et al., 1999; Hamid et al., 2005). In a similar manner, accelerated proliferation of SLFs induced by the factors secreted by MSCs may result from increased cell proliferation and resistance to apoptosis. In addition, SLFs cultured with or without MSC conditioned medium also showed differential expression of several genes related to extracellular matrix and adhesion molecules (Table III). *Thbs1* and *MMP11*, which were downregulated in SLFs with MSC stimulation, are involved in apoptosis (Friedl et al., 2002) and cell proliferation (Deng et al., 2005), respectively. The effects of these molecules on SLFs should be investigated in a future study. In the 3NP model, rats with injury to the SL had a higher rate of MSC invasion than did those without injury (Kamiya et al., 2007). Our results here show that factors secreted by MSCs induced SLF proliferation. Thus we speculate that the transplanted MSCs in the injured SL might promote SLFs to regenerate, leading to hearing recovery. In addition, we found that SLF conditioned medium promoted the transdifferentiation of MSCs into SLF-like cells. Whether transplanted MSCs in vivo have this ability to transdifferentiate into SLF-like cells must be determined in the future. MSCs expressed the gap junction protein Cx31, which is related to hearing loss (Mhatre et al., 2003), regardless of exposure to SLF conditioned medium (data not shown). In the injured SL, transplanted MSCs protrude toward neighboring fibrocytes and express the cochlear gap junction protein connexin 26 (Kamiya et al., 2007). Gap junctions between cochlear fibrocytes play an important role in the cochlear potassium recycling system, and a disrupted gap junction network, which occurs with the loss of SLFs, is thought to be one of the main causes of hearing loss (Lopez-Bigas et al., 2002). Taken together, these data suggest that the expression of gap junctions on MSCs is likely to play a role in reorganizing the gap junction network that occurs with the loss of SLFs.

CONCLUSIONS

Our results suggest that two mechanisms of hearing recovery occur in the damaged SL after transplantation of MSCs into the inner ear. One is that the transplanted MSCs transdifferentiate into SLF-like cells that compensate for the lost SLFs. The other is that the transplanted MSCs stimulate the proliferation and regeneration of the host SLFs. In this study, several candidate molecules that might be involved in these mechanisms were detected, and the role of TGF-β signaling in the proliferation of SLFs was verified. Further elucidation of key molecules in these mechanisms may lead to the establishment of a new therapeutic approach for sensorineural hearing loss.

ACKNOWLEDGMENTS

We thank Susumu Nakagawa for technical assistance.

REFERENCES

Achouche J, Wu AH, Liu DS, Huy PTB. 1991. Primary culture of strial marginal cells of guinea-pig cochlea—growth, morphological features, and characterization. Ann Otol Rhinol Laryngol 100:999–1006.

Baserga R. 1985. The biology of cell reproduction. Cambridge, MA: Harvard University Press. 251 p.

Benzeev A. 1985. Cell-density and cell shape-related regulation of vimentin and cytokeratin synthesis-inhibition of vimentin synthesis and appearance of a new 45-kD cytokeratin in dense epithelial-cell cultures. Exp Cell Res 157:520–532.

Bitar M, Brown RA, Salih V, Kidane AG, Knowles JC, Nazhat SN. 2008. Effect of cell density on osteoblastic differentiation and matrix degradation of biomimetic dense collagen scaffolds. Biomacromolecules 9:129–135.

Boland GM, Perkins G, Hall DJ, Tuan RS. 2004. Wnt 3a promotes proliferation and suppresses osteogenic differentiation of adult human mesenchymal stem cells. J Cell Biochem 93:1210–1230.

Bouillet P, OuladAbdelghani M, Ward SJ, Bronner S, Chambon P, Dolle P. 1996. A new mouse member of the Wnt gene family, mWnt-8, is expressed during early embryogenesis and is ectopically induced by retinoic acid. Mech Dev 58:141–152.

Bowers RR, Lane MD. 2007. A role for bone morphogenetic protein-4 in adipocyte development. Cell Cycle 6:385–389.

Bowman PD, Rarey K, Rogers C, Goldstein GW. 1985. Primary culture of capillary endothelial-cells from the spiral ligament and stria vasculars of bovine inner ear retention of several endothelial-cell properties in vitro. Cell Tissue Res 241:479–486.

Cho HH, Kim SH, Kim YG, Kim YC, Koller H, Camblor MA, Hong SB. 2000. Synthesis and characterization of gallosilicate molecular sieves with high gallium contents: examples of structure direction exerted by gallium. Chem Mater 12:2292–2300.

De Boer J, Wang HJ, Van Blitterswijk C. 2004. Effects of Wnt signaling on proliferation and differentiation of human mesenchymal stem cells. Tissue Eng 10:393–401.

Delprat B, Ruel J, Guitton MJ, Hamard G, Lenoir M, Pujol R, Puel JL, Brabet P, Hamel CP. 2005. Deafness and cochlear fibrocyte alterations in mice deficient for the inner ear protein otospiralin. Mol Cell Biol 25:847–853.

Deng H, Guo RF, Li WM, Zhao M, Lu YY. 2005. Matrix metalloproteinase 11 depletion inhibits cell proliferation in gastric cancer cells. Biochem Biophys Res Commun 326:274–281.

Dormady SP, Bashayan O, Dougherty R, Zhang XM, Basch RS. 2001. Immortalized multipotential mesenchymal cells and the hematopoietic microenvironment. J Hematother Stem Cell Res 10:125–140.

Ferrari S, Battini R, Kaczmarek L, Rittling S, Calabretta B, de Riel JK, Philiponis V, Wei JF, Baserga R. 1986. Coding sequence and growth regulation of the human vimentin gene. Mol Cell Biol 6:3614–3620.

Freter S, Muta Y, Mak S-S, Rinkwitz S, Ladher RK. 2008. Progressive restriction of otic fate: the role of FGF and Wnt in resolving inner ear potential. Development 135:3415–3424.

Friedl P, Vischer P, Freyberg MA. 2002. The role of thrombospondin-1 in apoptosis. Cell Mol Life Sci 59:1347–1357.

Gratton MA, Schulte BA, Hazen-Martin DJ. 1996. Characterization and development of an inner ear type I fibrocyte cell culture. Hear Res 99:71–78.

Guo L, Kawazoe N, Fan Y, Ito Y, Tanaka J, Tateishi T, Zhang X, Chen G. 2008. Chondrogenic differentiation of human mesenchymal stem cells on photoreactive polymer-modified surfaces. Biomaterials 29:23–32.

Hamid T, Malik MT, Kakar SS. 2005. Ectopic expression of PTTGI/securin promotes tumorigenesis in human embryonic kidney cells. Mol Cancer 4.

Hequembourg S, Liberman MC. 2001. Spiral ligament pathology: a major aspect of age-related cochlear degeneration in C57BL/6 mice. J Assoc Res Otol 2:118–129.

Hirose K, Liberman MC. 2003. Lateral wall histopathology and endocochlear potential in the noise-damaged mouse cochlea. J Assoc Res Otol 4:339–352.

Hirose M, Hashimoto H, Iga J, Shintani N, Nakanishi M, Arakawa N, Shimada T, Baba A. 2006. Inhibition of self-renewal and induction of neural differentiation by PACAP in neural progenitor cells. Vip Pacap Rel Peptides Gene Ther 1070:342–347.

Hoya N, Okamoto Y, Kamiya K, Fujii M, Matsunaga T. 2004. A novel animal model of acute cochlear mitochondrial dysfunction. Neuroreport 15:1597–1600.

Huang SS, Huang JS. 2005. TGF-beta control of cell proliferation. J Cell Biochem 96:447–462.

Islam MQ, Meirelles LD, Nardi NB, Magnusson P, Islam K. 2006. Polyethylene glycol-mediated fusion between primary mouse mesenchymal stem cells and mouse fibroblasts generates hybrid cells with increased proliferation and altered differentiation. Stem Cells Dev 15:905–919.

Jung GA, Yoon JY, Moon BS, Yang DH, Kim HY, Lee SH, Bryja V, Arenas E, Choi KY. 2008. Valproic acid induces differentiation and inhibition of proliferation in neural progenitor cells via the beta-catenin-Ras-ERK-p21(Cip/WAF1) pathway. BMC Cell Biol 9.

Kakar SS, Jennes L. 1999. Molecular cloning and characterization of the tumor transforming gene (TUTR1): a novel gene in human tumorigenesis. Cytogenet Cell Genet 84:211–216.

Kamiya K, Fujinami Y, Hoya N, Okamoto Y, Kouike H, Komatsuzaki R, Kusano R, Nakagawa S, Satoh H, Fujii M, Matsunaga T. 2007. Mesenchymal stem cell transplantation accelerates hearing recovery through the repair of injured cochlear fibrocytes. Am J Pathol 171:214–226.

Katoh M. 2005. Comparative genomics on Wnt8a and Wnt8b genes. Int J Oncol 26:1129–1133.

Kingsley DM. 1994. The TGF-beta superfamily—new menbers, new receptors, and new genetic tests of function in different organisms. Genes Dev 8:133–146.

Kuijpers W, Tonnaer EL, Peters TA, Ramaekers FC. 1992. Developmentally-regulated coexpression of vimentin and cytokeratins in the rat inner ear. Hear Res 62:1–10.

Lai YQ, Xin DQ, Bai JH, Mao ZB, Na YQ. 2007. The important anti-apoptotic role and its regulation mechanism of PTTG1 in UV-induced apoptosis. J Biochem Mol Biol 40:966–972.

Lang H, Schulte BA, Schmiedt RA. 2003. Effects of chronic furosemide treatment and age on cell division in the adult gerbil inner ear. J Assoc Res Otol 4:164–175.

Laping NJ, Grygielko E, Mathur A, Butter S, Bomberger J, Tweed C, Martin W, Fornwald J, Lehr R, Harling J, Gaster L, Callahan JF, Olson BA. 2002. Inhibition of transforming growth factor (TGF)-beta 1-induced extracellular matrix with a novel inhibitor of the TGF-beta type I receptor kinase activity: SB-431542. Mol Pharmacol 62:58–64.

Lee IC, Wang JH, Lee YT, Young TH. 2007. The differentiation of mesenchymal stem cells by mechanical stress or/and co-culture system. Biochem Biophys Res Commun 352:147–152.

Lopez-Bigas N, Arbones ML, Estivill X, Simonneau L. 2002. Expression profiles of the connexin genes, Gjb1 and Gjb3, in the developing mouse cochlea. Gene Express Pattern 2:113–117.

Massague J. 1990. The transforming growth factor beta family. Annu Rev Cell Biol 6:597–641.

Massague J. 1998. TGF-beta signal transduction. In: Richardson CC, editor. Annu Rev Biochem. p 753–791.

Matsuyama S, Iwadate M, Kondo M, Saitoh M, Hanyu A, Shimizu K, Aburatani H, Mishima HK, Imamura T, Miyazono K, Miyazawa K. 2003. SB-431542 and Gleevec inhibit transforming growth factor-13-induced proliferation of human osteosarcoma. Cancer Res 63:7791–7798.

McBeath R, Pirone DM, Nelson CM, Bhadriraju K, Chen CS. 2004. Cell shape, cytoskeletal tension, and RhoA regulate stem cell lineage commitment. Dev Cell 6:483–495.

McCartney-Francis NL, Frazier-Jessen M, Wahl SM. 1998. TGF-beta: a balancing act. Int Rev Immunol 16:553–580.

Melichar I, Gitter AH. 1992. Ultrastructure of cultured marginal cells of the guinea pig cochlea. Acta Otolaryngol 112:762–766.

Mhatre AN, Weld E, Lalwani AK. 2003. Mutation analysis of connexin 31 (GJB3) in sporadic non-syndromic hearing impairment. Clin Genet 63:154–159.

Minowa O, Ikeda K, Sugitani Y, Oshima T, Nakai S, Katori Y, Suzuki M, Furukawa M, Kawase T, Zheng Y, Ogura M, Asada Y, Watanabe K, Yamanaka H, Gotoh S, Nishi-Takeshima M, Sugimoto T, Kikuchi T, Takasaka T, Noda T. 1999. Altered cochlear fibrocytes in a mouse model of DFN3 nonsyndromic deafness. Science 285:1408–1411.

Mizutari K, Nakagawa S, Mutai H, Fujii M, Ogawa K, Matsunaga T. 2011. Late-phase recovery in the cochlear lateral wall following severe degeneration by acute energy failure. Brain Res 1419:1–11.

Mohammadi M, McMahon G, Sun L, Tang C, Hirth P, Yeh BK, Hubbard SR, Schlessinger J. 1997. Structures of the tyrosine kinase domain of fibroblast growth factor receptor in complex with inhibitors. Science 276:955–960.

Mutai H, Nagashima R, Fujii M, Matsunaga T. 2009. Mitotic activity and specification of fibrocyte subtypes in the developing rat cochlear lateral wall. Neuroscience 163:1255–1263.

Neuhuber B, Swanger SA, Howard L, Mackay A, Fischer I. 2008. Effects of plating density and culture time on bone marrow stromal cell characteristics. Exp Hematol 36:1176–1185.

Ohyama T, Mohamed OA, Taketo MM, Dufort D, Groves AK. 2006. Wnt signals mediate a fate decision between otic placode and epidermis. Development 133:865–875.

Okamoto Y, Hoya N, Kamiya K, Fujii M, Ogawa K, Matsunaga T. 2005. Permanent threshold shift caused by acute cochlear mitochondrial dysfunction is primarily mediated by degeneration of the lateral wall of the cochlea. Audiol Neurootol 10:220–233.

Otto TC, Lane MD. 2005. Adipose development: from stem cell to adipocyte. Crit Rev Biochem Mol Biol 40:229–242.

Pelton RW, Saxena B, Jones M, Moses HL, Gold LI. 1991. Immunohistochemical localization of TGF-beta1, TGF-beta2, and TGF-beta 3 in the mouse embryo expression patterns suggest mutiple roles during embryonic development. J Cell Biol 115:1091–1105.

Pickles JO. 2001. The expression of fibroblast growth factors and their receptors in the embryonic and neonatal mouse inner ear. Hear Res 155:54–62.

Rarey KE, Patterson K. 1989. Estabilishment of innerear epithelial cell culture—isolation, growth and characterization. Hear Res 38:277–287.

Roberson DW, Rubel EW. 1994. Cell division in the gerbil cochlea after acoustic trauma. Am J Otol 15:28–34.

Rose RA, Jiang H, Wang X, Helke S, Tsoporis JN, Gong N, Keating SCJ, Parker TG, Backx PH, Keating A. 2008. Bone marrow-derived mesenchymal stromal cells express cardiac-specific markers, retain the stromal phenotype, and do not become functional cardiomyocytes in vitro. Stem Cells 26:2884–2892.

Ruben R. 1967. Development of the inner ear of the mouse: a radioautographic study of terminal mitoses. Acta Otolaryngol Suppl 220:1–44.

Schulte BA, Steel KP. 1994. Expression of alpha-subunit and beta-subunit isoforms of Na,K-ATPase in the mouse inner-ear and changes with mutations at the W-V or Sld loci. Hear Res 78:65–76.

Sensebe L, Deschaseaux M, Li J, Herve P, Charbord P. 1997. The broad spectrum of cytokine gene expression by myoid cells from the human marrow microenvironment. Stem Cells 15:133–143.

Shi YG, Massague J. 2003. Mechanisms of TGF-beta signaling from cell membrane to the nucleus. Cell 113:685–700.

Song SJ, Jeon O, Yang HS, Ran DK, Kim BS. 2007. Effects of culture conditions on osteogenic differentiation in human mesenchymal stem cells. J Microbiol Biotechnol 17:1113–1119.

Spicer SS, Schulte BA. 1991. Differentiation of inner-ear fibrocyties according to their ion-transport related activity. Hear Res 56:53–64.

Spicer SS, Schulte BA. 1996. The fine structure of spiral ligament cells relates to ion return to the stria and varies with place-frequency. Hear Res 100:80–100.

Spicer SS, Schulte BA. 2002. Spiral ligament pathology in quiet-aged gerbils. Hear Res 172:172–185.

Suko T, Ichimiya I, Yoshida K, Suzuki M, Mogi G. 2000. Classification and culture of spiral-ligament fibrocytes from mice. Hear Res 140:137–144.

Takahashi T, Kimura RS. 1970. The ultrastructure of the spiral ligament in the Rhesus monkey. Acta Otolaryngol 69:46–60.

Tsuprun V, Santi P. 1999. Ultrastructure and immunohistochemical identification of the extracellular matrix of the chinchilla cochlea. Hear Res 129:35–49.

Wang YQ, Sizeland A, Wang XF, Sassoon D. 1995. Restricted expression of type-II TGF-beta receptor in murine embryonic development suggest a central role in tissue modeling and CNS patterning. Mech Dev 52:275–289.

Wangemann P. 2002. K^+ cycling and the endocochlear potential. Hear Res 165:1–9.

Weber PC, Cunningham CD, Schulte BA. 2001. Potassium recycling pathways in the human cochlea. Laryngoscope 111:1156–1165.

Yian C, Moon SK, Jin SJ, Webster P, Rhim JS, Andalibi A, Lim DJ. 2006. Characterization of rat spiral ligament cell line immortalized by adenovirus 12-simian virus 40 hybrid virus. Ann Otol Rhinol Laryngol 115:930–938.

Zhang X, Horwitz GA, Prezant TR, Valentini A, Nakashima M, Bronstein MD, Melmed S. 1999. Structure, expression, and function of human pituitary tumor-transforming gene (PTTG). Mol Endocrinol 13:156–166.

Biochemical and Biophysical Research Communications 432 (2013) 475–479

Contents lists available at SciVerse ScienceDirect

Biochemical and Biophysical Research Communications

journal homepage: www.elsevier.com/locate/ybbrc

Moderate hearing loss associated with a novel KCNQ4 non-truncating mutation located near the N-terminus of the pore helix

Takahisa Watabe [a], Tatsuo Matsunaga [b,*], Kazunori Namba [b], Hideki Mutai [b], Yasuhiro Inoue [a], Kaoru Ogawa [a]

[a] Department of Otolaryngology, Head and Neck Surgery, Keio University, School of Medicine, 35 Shinanomachi, Shinjuku, Tokyo 160-8582, Japan
[b] The Laboratory of Auditory Disorders, National Institute of Sensory Organs, National Tokyo Medical Center, 2-5-1 Higashigaoka, Meguro, Tokyo 152-8902, Japan

ARTICLE INFO

Article history:
Received 28 January 2013
Available online 9 February 2013

Keywords:
KCNQ4
Nonsyndromic hearing loss
Dominant negative effect
Haploinsufficiency
Molecular modeling

ABSTRACT

Genetic mutation is one of the causative factors for idiopathic progressive hearing loss. A patient with late-onset, moderate, and high-frequency hearing loss was found to have a novel, heterozygous *KCNQ4* mutation, c.806_808delCCT, which led to a p.Ser260del located between S5 and the pore helix (PH). Molecular modeling analysis suggested that the p.Ser269del mutation could cause structural distortion and change in the electrostatic surface potential of the *KCNQ4* channel protein, which may impede K+ transport. The present study supports the idea that a non-truncating mutation around the N-terminus of PH may be related to moderate hearing loss.

1. Introduction

Currently, 50 loci and 27 responsible genes for autosomal dominant non-syndromic hearing loss (DFNA) have been identified [1]. *KCNQ4* is one gene that can cause DFNA, type 2 (DFNA2, OMIM: 600101) [2,3]. Patients with mutations in this gene present progressive sensorineural hearing loss starting in the high frequency range. *KCNQ4* (OMIM: 603537) is a voltage-gated KQT-like potassium channel. It modulates the resting membrane potential of the outer hair cells, a type of auditory sensory cell. A functional *KCNQ4* channel consists of four subunits. Each subunit contains six putative domains that span the cellular membrane (S1–S6), a K+-selective pore region consisting of S5, S6, a pore helix (PH), and a pore-loop (P-loop) domain, and N- and C-terminal regions [3].

So far, 11 missense mutations, one nonsense mutation, and three small deletion mutations in *KCNQ4* have been reported to be associated with hearing loss. Understanding the molecular pathology resulting from each *KCNQ4* mutation would be beneficial in predicting the clinical course of KCNQ-related hearing loss. *KCNQ4* mutations can be divided into non-truncating and truncating mutations (Table 1). Most of the *KCNQ4* non-truncating mutations in the pore region are associated with severe hearing loss, except for a non-truncating mutation at the N-terminus of PH, p.Tyr270His, which has been associated with moderate hearing loss [13]. In an electrophysiological study, co-expression of wild-type *KCNQ4* with each non-truncating mutation associated with severe hearing loss, including p.Leu274His, p.Trp276Ser, p.Leu281-Ser, p.Gly285Cys, p.Gly285Ser, p.Gly296Ser, p.Gly321Ser, and p.Gly322_Leu327del, has been shown to result in significantly reduced or non-detectable current [14]. These results indicate that the severe hearing loss in patients carrying these heterozygous mutations is due to a dominant negative effect. On the other hand, the protein products of two *KCNQ4*-truncating mutations, p.Gln71SerfsX138 and p.Gln71fs, lack structural motifs, such as transmembrane domains, and are probably not synthesized from these alleles. Moderate hearing loss in patients carrying these mutations in the heterozygous allele has been considered to be due to haploinsufficiency [3,11].

We identified a novel heterozygous *KCNQ4* non-truncating mutation, c.806_808delCCT, that leads to deletion of a serine residue at position 269 (p.Ser269del), located in the region between S5 and the PH of the protein. Unlike other patients with *KCNQ4* non-truncating mutations, the patient who carried this mutation presented moderate hearing loss. Previously, we reported that a patient having *KCNQ4* with p.Try270His, which is located next to Ser269, showed moderate hearing loss [13], raising the possibility that mutation at or proximal to the N-terminus of PH is associated

Abbreviations: DFNA2, nonsyndromic autosomal dominant sensorineural deafness type 2; *KCNQ4*, potassium voltage-gated channel; KQT-like subfamily, member 4; ABR, auditory brainstem response.

* Corresponding author. Fax: +81 3 3412 9811.
E-mail address: matsunagatatsuo@kankakuki.go.jp (T. Matsunaga).

0006-291X/$ - see front matter © 2013 Elsevier Inc. All rights reserved.
http://dx.doi.org/10.1016/j.bbrc.2013.01.118

Table 1
KCNQ4 mutations affecting the pore region of the channel protein in DFNA2 families.

	Exon		Nucleotide	Amino acid	Protein domain	Onset (y)	Progression	Severity	Mechanism	Refs.
Non-truncating mutation	5	Missense	c.778G>A	p.Glu260Lys	S5	1–20	Yes	SV	Unknown	[9]
	5		c.785A>T	p.Asp262Val	S5-PH	1–20	Yes	SV	Unknown	[9]
	5		c.808T>C	p.Tyr270His	N-terminus of PH	0	Yes	MD	Unknown	[13]
	5		c.821T>A	p.Leu274His	PH	1–20	Yes	SV	D.N.E.	[12]
	5		c.827G>C	p.Trp276Ser	PH	1–20	Yes	SV	D.N.E.	[3–5]
	6		c.842T>C	p.Leu281Ser	PH	1–20	Yes	SV	D.N.E.	[6]
	6		c.853G>T	p.Gly285Cys	P-loop	1–20	Yes	SV	D.N.E.	[3]
	6		c.853G>A	p.Gly285Ser	P-loop	1–20	Yes	SV	D.N.E.	[2]
	6		c.859G>C	p.Gly287Arg	P-loop	1–20	Yes	SV	D.N.E.	[7]
	6		c.886G>A	p.Gly296Ser	S6	1–20	Yes	SV	D.N.E.	[8]
	7		c.961G>A	p.Gly321Ser	S6	1–20	Yes	SV	D.N.E.	[3]
	4	Deletion	c.664_681del18	p.Gly322_Leu327del	S5	1–20	Yes	SV	D.N.E.	[10]
	5		c.806_808del3	p.Ser269del	S5-PH	1–20	Yes	MD	See discussion	This study
Truncating mutation	1	Deletion	c.211del1	p.Gln71SerfsX138	N-terminal cytoplasmic	Unknown	Yes	MD	H.I.?	[11]
	1		c.212_224del13	p.Gln71fs	N-terminal cytoplasmic	1–20	Yes	MD	H.I.?	[3]
	5	Nonsense	c.725G>A	p.Trp242X	S5	1–20	Unknown	SV	Unknown	[9]

SV: severe, MD: moderate D.N.E.: dominant negative effect, H.I.: haploinsufficiency, PH: pore helix.

with moderate hearing loss. In this study, we used molecular modeling to elucidate the molecular mechanism underlying moderate hearing loss associated with *KCNQ4* harboring the p.Ser269del mutation.

2. Materials and methods

2.1. Subjects

All procedures were approved by the Ethics Review Committee of National Mie Hospital and National Tokyo Medical Center, and were conducted after written informed consent had been obtained from each individual.

2.2. Clinical analysis

Hearing level was measured by pure tone audiometry and evaluated by averaging four frequencies, 500, 1000, 2000, and 4000 Hz in the better hearing ear and was classified according to the criteria of GENDEAF (moderate, 41–70 dB; severe, 71–95 dB) [1]. Clinical information, such as age of onset and presence of progression, was gathered from the medical records. Computed tomography (CT) and magnetic resonance imaging (MRI) were done to check whether the patient had an inner ear anomaly and/or retrocochlear disease. Auditory brainstem response (ABR) and distortion product otoacoustic emission (DPOAE) were also examined to evaluate inner ear function.

2.3. Genetic analysis

KCNQ4 was selected as the candidate gene on the basis of clinical features, including onset of hearing loss, audiogram patterns, imaging studies, and hereditary pattern [15]. Prior to this study, the patient was confirmed to have neither GJB2 mutations, the most common causative gene of hereditary hearing loss, nor mitochondrial m.1555A>G and m.3243A>G mutations. Genomic DNA was extracted from blood samples using the Gentra Puregene Blood kit (QIAGEN, Hamburg, Germany). PCR primers specific for *KCNQ4* (GenBank NG_008139, NCBI Build37.1) were selected from the resequencing amplicon probe sets (NCBI). All of the exons, together with the flanking intronic regions, of *KCNQ4* were analyzed by bidirectional sequencing using an ABI 3730 Genetic Analyzer (Applied Biosystems, CA, USA) and the ABI Prism Big Dye Terminator Cycle Sequencing kit (Applied Biosystems). The sequences were characterized using SeqScape software v.2.6 (Applied Biosystems) and DNASIS Pro (Hitachisoft, Tokyo, Japan). Control DNA was obtained from 96 Japanese subjects with normal hearing.

2.4. Molecular model analysis

To predict the effects of the mutation on the KCNQ4 channel, molecular modeling of KCNQ4 was performed as previously described [13]. The crystal structure of Kv1.2 (PDB ID: 3LUT, chain B) [16] was used as the structural template for modeling of the *KCNQ4* sequence based on sequence homology as determined through Gapped BLAST [17] and PDBsum [18]. The pore regions of wild-type KCNQ4 and the p.Ser269del mutation were modeled using SWISS-MODEL Workspace [19] and validated using the Verify 3D Structure Evaluation server [20,21]. The models were each superimposed onto Kv1.2 using Chimera [22] to visualize ribbon models with electrostatic surface potentials and the hydrogen bonds of either wild-type KCNQ4 or KCNQ4 with the p.Ser269del mutation.

3. Results

3.1. Clinical features

The proband was a 25-years-old female in a pedigree of autosomal dominant progressive hearing loss (Fig. 1A). She has become conscious of progressive bilateral hearing loss, since she has become 20 years-old. At 24 years-old, severe mixed hearing loss with high frequency dominance was found in the right ear by pure tone audiometry. An air-bone gap was considered to have resulted from an operation for a right cholesteatoma at 8 years of age. Moderate sensorineural hearing loss with high frequency dominance was found in the left ear (Fig. 1B). No other symptoms accompanying the hearing loss were identified. ABR showed a threshold of 90 dB in the left ear, and no response at 90 dB in the right ear. DPOAE showed a response only at 1000 Hz in the left ear and no response in the right ear. CT and MRI failed to reveal deformity of the inner ear or structural abnormality in the central auditory pathway.

3.2. Novel mutation of KCNQ4

Sequencing analysis of *KCNQ4* from the patient identified a heterozygous deletion of three nucleotides, CCT, at position 806–808 (c.806_808delCCT). The deletion mutation causes a change of amino acid residues from Ser268-Ser269-Tyr270 to Ser268-Tyr269 (p.Ser269del) without a frameshift (Fig. 2A). Ser269 was located

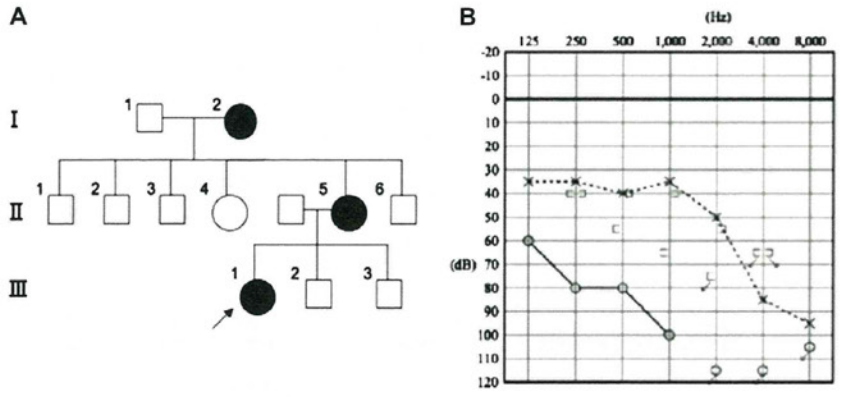

Fig. 1. Clinical information. (A) Pedigree of a family carrying heterozygous *KCNQ4* with the c.806_808delCCT (p.Ser269del) mutation. Individuals with hearing loss are indicated by filled symbols. The arrow indicates the proband. (B) Pure tone audiogram from the proband at 25 years old. Open circles with line: air conduction thresholds of the right ear; x with dotted line: air conduction thresholds of the left ear; left bracket: bone conduction thresholds of the right ear; right bracket: bone conduction thresholds of the left ear. Arrows indicate the non-detectable hearing level by profound hearing loss.

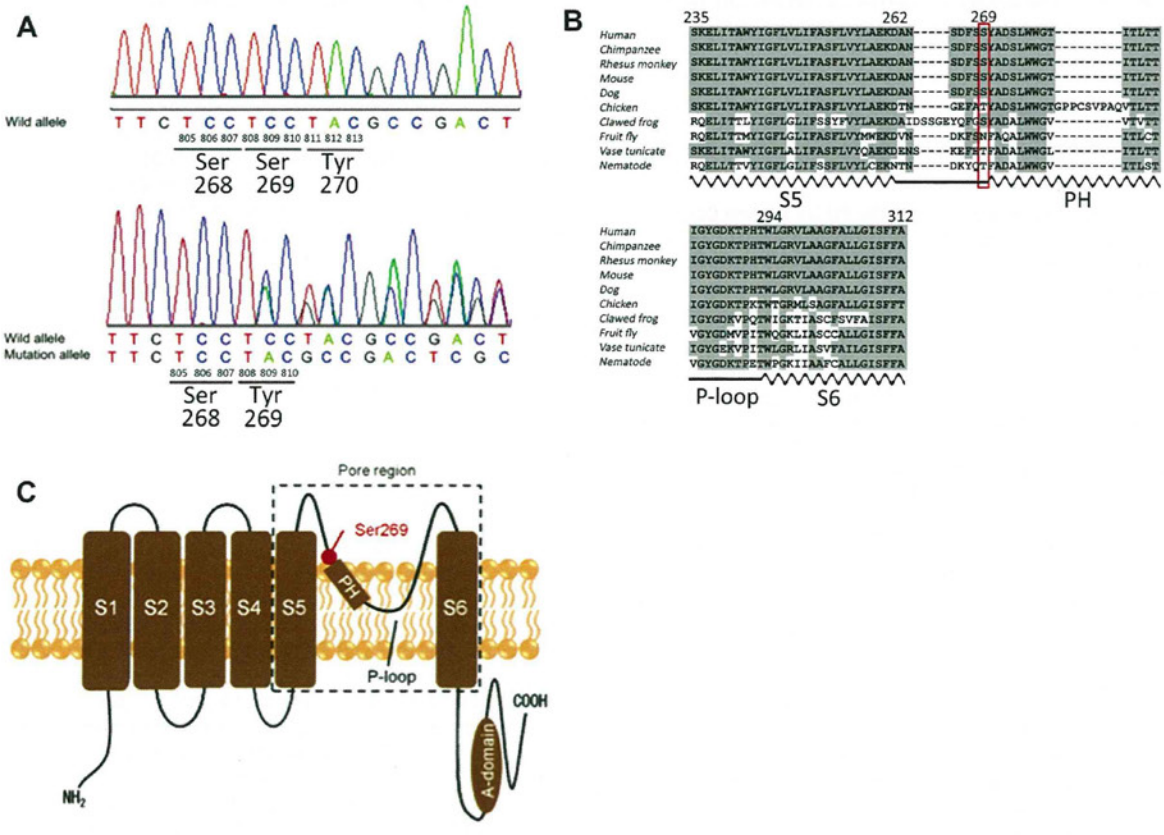

Fig. 2. Partial electrophoretogram of exon 5 of *KCNQ4* with the partial protein sequence for *KCNQ4*. (A) A partial electrophoretogram of exon 5 of *KCNQ4* from an individual with normal hearing (above) and the proband with the heterozygous c.806–808delCCT mutation (below). The positions of the heterozygotic deletion of CCT at 806–808 and the resulting amino acid deletion (p.Ser269del) are indicated. (B) Sequences of the orthologous *KCNQ4* pore region are aligned. Positions highlighted in gray indicate the residues identical to human *KCNQ4*. The position of Ser269 is enclosed by a red square. The positions of S5, pore helix (PH), S6 (wavy lines) and the P-loop (straight line) are shown below the sequences. (C) Schematic topology of *KCNQ4*. Putative domains, including transmembrane regions (S1-S6), channel pore region, PH, P-loop, and A-domain are indicated. Position of Ser269 is indicated by a red circle. (For interpretation of the references to color in this figure legend, the reader is referred to the web version of this article.)

in the region between the putative S5 and PH, a highly conserved region among animal species (Fig. 2B and C). This mutation was found neither on the Exome Variant Server [23] nor in the control group of 96 unrelated Japanese individuals with normal hearing.

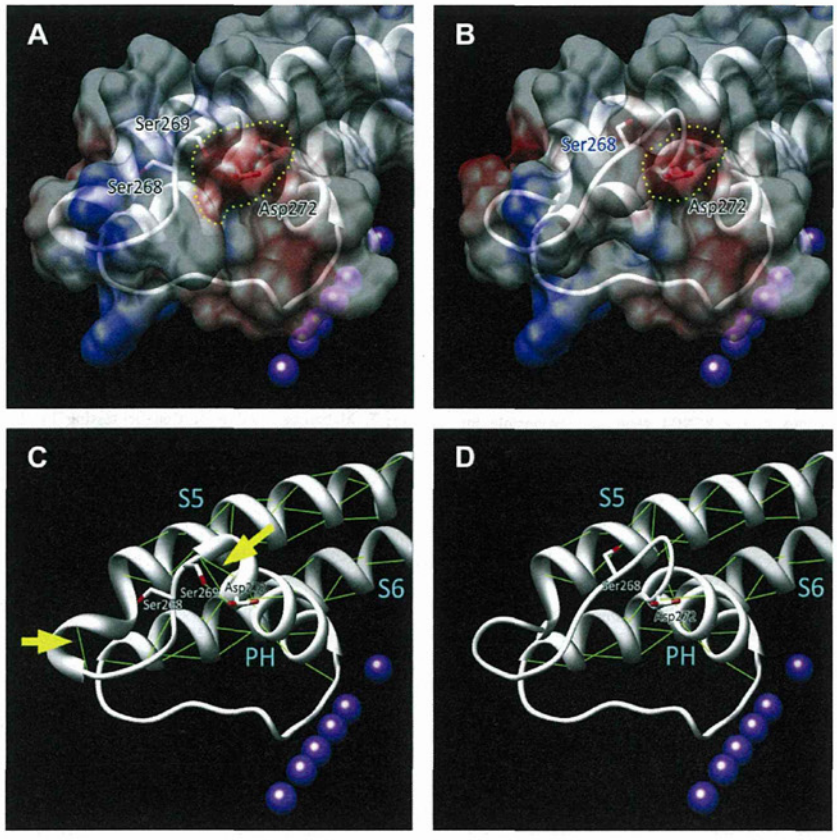

Fig. 3. Partial structural model of KCNQ4 and the p.Ser269del mutation. (A and B) The ribbon models of (A) wild-type KCNQ4 subunit and (B) KCNQ4 subunit with the p.Ser269del mutation overlaid with their corresponding electrostatic surface potential. Red or blue area: negatively or positively charged residues, yellow dot circle: negatively charged surface potential on the N-terminal region of the pore helix (PH). (C and D) Ribbon models of (C) wild-type KCNQ4 and (D) KCNQ4 with the p.Ser269del mutation. Green lines: putative hydrogen bonds; yellow arrows: hydrogen bonds within S5 and PH; purple spheres: potassium ions. (For interpretation of the references to color in this figure legend, the reader is referred to the web version of this article.)

3.3. Predicted structural change in KCNQ4 caused by the p.Ser269del mutation

The ribbon model of the wild-type KCNQ4 subunit overlaid with the corresponding electrostatic surface potential demonstrated that the surface of the N-terminal region of PH is negatively charged because of the negatively charged side chains of Ser269 and Asp272 (Fig. 3A). The model of KCNQ4 with the p.Ser269del mutation demonstrated reduction of the negatively charged surface area in this region (Fig. 3B). Reduction of the electrostatic surface potential in this area has been predicted to impede K+ transport because of the long range electrostatic attractive force between PH and K+ [13]. In addition, hydrogen bonds on the C-terminus of S5 and the N-terminus of PH of wild-type KCNQ4 (Fig. 3C, yellow arrows) were absent in KCNQ4 with the Ser269del mutation (Fig. 3D). Loss of the hydrogen bonds around the N-terminus of PH resulted in shortening of the PH and was attributed to destabilization of α-helix formation [24]. The disrupted helices would affect the structural stability of the pore region and lead to abnormal channel function.

4. Discussion

Most of the *KCNQ4* non-truncating mutations affecting the pore region are associated with severe hearing loss. However, we found that the non-truncating p.Tyr270His [14] and p.Ser269del mutations were associated with moderate hearing loss. *KCNQ4* mutations at or proximal to the N-terminus of PH are suggested to be associated with moderate hearing loss, because this site is predicted to have relatively smaller influence than other pore regions, such as S5, S6, the central region of PH, and the P-loop, on KCNQ4 channel function.

The molecular pathology associated with the p.Ser269del mutation, demonstrated in silico, indicates a reduction in the negatively charged electrostatic surface potential and structural distortion of the pore region by the mutated KCNQ4, which may explain the associated moderate hearing loss. The molecular mechanism in this case is likely to be a mild dominant negative effect resulting from the relatively small influence of *KCNQ4* with the p.Ser269del mutation on the normal channel subunit. However, another possibility is haploinsufficiency resulting from the loss of function of *KCNQ4* with the p.Ser269del mutation. This scenario, which would not affect the functioning of the other channel subunits, cannot be excluded.

5. Conclusion

We found a novel heterozygous *KCNQ4* mutation, c.806_808delCCT (p.Ser269del), in a pedigree with progressive and moderate hearing loss. Molecular modeling analysis of this mutation demonstrated that changes in electrostatic surface potential and structural distortion could be relevant to the pathology underlying

auditory dysfunction. Mutations at or proximal to the N-terminus of the PH of the KCNQ4 channel might cause mild molecular dysfunction and be associated with moderate hearing loss.

Acknowledgment

This study was supported by a Grant-in-Aid for Clinical Research from the National Hospital Organization.

References

[1] <http://hereditaryhearingloss.org/> (accessed September 2012).
[2] C. Kubisch, B.C. Schroeder, T. Friedrich, B. Lütjohann, A. El Amraoui, S. Marlin, C. Petit, T.J. Jentsch, KCNQ4, a novel potassium channel expressed in sensory outer hair cells, is mutated in dominant deafness, Cell 96 (1999) 437–446.
[3] P.J. Coucke, P. Van Hauwe, P.M. Kelley, H. Kunst, I. Schatteman, D. Van Velzen, J. Meyers, R.J. Ensink, M. Verstreken, F. Declau, H. Marres, K. Kastury, S. Bhasin, W.T. McGuirt, R.J. Smith, C.W. Cremers, P. Van de Heyning, P.J. Willems, S.D. Smith, G. Van Camp, Mutations in the KCNQ4 gene are responsible for autosomal dominant deafness in four DFNA2 families, Hum. Mol. Genet. 8 (1999) 1321–1328.
[4] J. Akita, S. Abe, H. Shinkawa, W.J. Kimberling, S. Usami, Clinical and genetic features of nonsyndromic autosomal dominant sensorineural hearing loss: KCNQ4 is a gene responsible in japanese, J. Hum. Genet. 46 (2001) 355–361.
[5] G. Van Camp, P.J. Coucke, J. Akita, E. Fransen, S. Abe, E.M. De Leenheer, P.L. Huygen, C.W. Cremers, S. Usami, A mutational hot spot in the KCNQ4 gene responsible for autosomal dominant hearing impairment, Hum. Mutat. 20 (2002) 15–19.
[6] Z. Talebizadeh, P.M. Kelley, J.W. Askew, K.W. Beisel, S.D. Smith, Novel Mutation in the KCNQ4 Gene in a large kindred with dominant progressive hearing loss, Hum. Mutat. 14 (1999) 493–501.
[7] J. Arnett, S.B. Emery, T.B. Kim, A.K. Boerst, K. Lee, S.M. Leal, M.M. Lesperance, Autosomal dominant progressive sensorineural hearing loss due to a novel mutation in the KCNQ4 gene, Arch. Otolaryngol. Head Neck Surg. 137 (2011) 54–59.
[8] A. Mencía, D. González-Nieto, S. Modamio-Høybjør, A. Etxeberría, G. Aránguez, N. Salvador, I. Del Castillo, A. Villarroel, F. Moreno, L. Barrio, M.A. Moreno-Pelayo, A novel KCNQ4 pore-region mutation (p.G296S) causes deafness by impairing cell-surface channel expression, Hum. Genet. 123 (2008) 41–53.
[9] M.S. Hildebrand, D. Tack, S.J. McMordie, A. DeLuca, I.A. Hur, C. Nishimura, P. Huygen, T.L. Casavant, R.J. Smith, Audioprofile-directed screening identifies novel mutations in KCNQ4 causing hearing loss at the DFNA2 locus, Genet. Med. 10 (2008) 797–804.
[10] J.I. Baek, H.J. Park, K. Park, S.J. Choi, K.Y. Lee, J.H. Yi, T.B. Friedman, D. Drayna, K.S. Shin, U.K. Kim, Pathogenic effects of a novel mutation (c.664_681del) in KCNQ4 channels associated with auditory pathology, Biochim. Biophys. Acta 2011 (1812) 536–543.
[11] F. Kamada, S. Kure, T. Kudo, Y. Suzuki, T. Oshima, A. Ichinohe, K. Kojima, T. Niihori, J. Kanno, Y. Narumi, A. Narisawa, K. Kato, Y. Aoki, K. Ikeda, T. Kobayashi, Y. Matsubara, A novel KCNQ4 one-base deletion in a large pedigree with hearing loss: implication for the genotype-phenotype correlation, J. Hum. Genet. 51 (2006) 455–460.
[12] P. Van Hauwe, P.J. Coucke, R.J. Ensink, P. Huygen, C.W. Cremers, G. Van Camp, Mutations in the KCNQ4 K+ channel gene, responsible for autosomal dominant hearing loss, cluster in the channel pore region, Am. J. Med. Genet. 93 (2000) 184–187.
[13] K. Namba, H. Mutai, H. Kaneko, S. Hashimoto, T. Matsunaga, In silico modeling of the pore region of a KCNQ4 missense mutant from a patient with hearing loss, BMC Res. Notes 5 (2012) 145.
[14] H.J. Kim, P. Lv, C.R. Sihn, E.N. Yamoah, Cellular and molecular mechanisms of autosomal dominant form of progressive hearing loss, DFNA2, J. Biol. Chem. 286 (2011) 1517–1527.
[15] T. Matsunaga, Value of Genetic testing in the ontological approach for sensorineural hearing loss, Keio J. Med. 58 (2009) 216–222.
[16] X. Chen, Q. Wang, F. Ni, J. Ma, Structure of the full-length shaker potassium channel Kv1.2 by normal-mode-based X-ray crystallographic refinement, Proc. Natl. Acad. Sci. USA 107 (2010) 11352–11357.
[17] S.F. Altschul, T.L. Madden, A.A. Schäffer, J. Zhang, Z. Zhang, W. Miller, D.J. Lipman, Gapped BLAST and PSI-BLAST: a new generation of protein database search programs, Nucleic Acids Res. 25 (1997) 3389–3402.
[18] R.A. Laskowski, Enhancing the functional annotation of PDB structures in PDBsum using key figures extracted from the literature, Bioinformatics 23 (2007) 1824–1827.
[19] <http://swissmodel.expasy.org/> (accessed November 2012).
[20] <http://nihserver.mbi.ucla.edu/Verify_3D> (accessed November 2012).
[21] K. Arnold, L. Bordoli, J. Kopp, T. Schwede, The SWISS-MODEL workspace: a web-based environment for protein structure homology modeling, Bioinformatics 22 (2006) 195–201.
[22] E.F. Pettersen, T.D. Goddard, C.C. Huang, G.S. Couch, D.M. Greenblatt, E.C. Meng, T.E. Ferrin, UCSF Chimera – a visualization system for exploratory research and analysis, J. Comput. Chem. 25 (2004) 1605–1612.
[23] <http://evs.gs.washington.edu/EVS/> (accessed August 2012).
[24] W.G. Hol, Effects of the alpha-helix dipole upon the functioning and structure of proteins and peptides, Adv. Biophys. 19 (1985) 133–165.

Acta Oto-Laryngologica, 2012; 132: 1178–1182

informa
healthcare

ORIGINAL ARTICLE

Mitochondrial DNA haplogroup associated with hereditary hearing loss in a Japanese population

TOMOFUMI KATO[1,2], NORIYUKI FUKU[2], YOSHIHIRO NOGUCHI[3], HARUKA MURAKAMI[4], MOTOHIKO MIYACHI[4], YURIKA KIMURA[1], MASASHI TANAKA[2] & KEN KITAMURA[3]

[1]*Otolaryngology, Tokyo Metropolitan Geriatric Hospital,* [2]*Genomics for Longevity and Health, Tokyo Metropolitan Institute of Gerontology,* [3]*Otolaryngology, Tokyo Medical and Dental University and* [4]*Health Promotion and Exercise, National Institute of Health and Nutrition, Tokyo, Japan*

Abstract

Conclusion: Haplogroup D4b, especially subhaplogroup D4b2, may be one of the modifiers associated with the phenotypic expression of hereditary hearing loss (HL). *Objectives:* The present study investigated the association between suspected hereditary HL and 12 major mtDNA haplogroups in a Japanese population. Besides the mutations of mitochondrial DNA, many modifiers including environmental factors and genetic polymorphisms are involved in HL. *Methods:* The subjects comprised 373 unrelated Japanese patients with suspected hereditary HL and 480 controls. Twenty of the 373 patients were excluded from the study because the m.1555A>G or the m.3243A>G mutation had been detected in them. The mitochondrial haplotypes were classified into 12 major Japanese haplogroups (i.e. F, B, A, N9a, N9b, M7a, M7b, G1, G2, D4a, D4b, and D5). The frequency of each haplogroup in patients with HL was compared with that of the controls using the chi-squared test. *Results:* The frequency of the HL patients carrying the mitochondrial haplogroup D4b was significantly higher than that of the controls (37/353 [10.5%] vs 31/480 [6.5%]; OR 1.70 [95% CI 1.03–2.79, $p = 0.036$]) and evidence for enhancement was found in subhaplogroup D4b2 (32/353 [9.1%] vs 24/480 [5%], OR 1.89 [95% CI 1.09–3.28, $p = 0.021$]).

Keywords: *Mitochondrial DNA polymorphisms, modifiers, haplotype*

Introduction

Sensorineural hearing loss (HL) is the most common sensory disorder in humans, affecting about 1.9 per 1000 children at birth; and the ratio of patients with HL increases with age [1]. It is assumed that patients with suspected hereditary HL include not only those carrying the pathogenic mutations but also those with a multitude of intrinsic and extrinsic factors [2]. In fact, previous studies have revealed that HL is correlated with genetic polymorphisms in somatic genes [3,4]. Many pathogenic mitochondrial DNA (mtDNA) mutations are well known to cause HL [5-7]. Just as in the case of genetic polymorphisms in somatic genes, it is natural to consider that mtDNA polymorphisms could be associated with the phenotypic expression of HL. However, no association study between mtDNA haplogroups and HL has been performed. In this study, we focused on the correlation between mitochondrial haplogroups (i.e., a set of tightly-linked mtDNA polymorphisms) and hereditary HL. We performed a case-control study on the association between 12 major mitochondrial haplogroups and suspected hereditary HL in a Japanese population, based on the comprehensive analysis of polymorphisms in the coding region of the mtDNA.

Correspondence: Tomofumi Kato, Otolaryngology, Tokyo Metropolitan Geriatric Hospital, 35-2 Sakaecho, Itabashi-ku, Tokyo, Japan. Tel: +81 3 39641141. Fax: +81 3 39641982. E-mail: tomofumi_kato@tmghig.jp

(Received 15 March 2012; accepted 6 May 2012)

ISSN 0001-6489 print/ISSN 1651-2251 online
DOI: 10.3109/00016489.2012.693624

Table I. Demographic features of the patients with hearing loss (HL).

Feature		Value
Sex	Male	144 (38.6%)
	Female	229 (61.4%)
Age at onset of HL (years)	Newborn or 0	31 (8.3%)
	1–3	23 (6.2%)
	4–10	80 (21.4%)
	11–20	43 (11.5%)
	21–30	39 (10.5%)
	31–40	50 (13.4%)
	41–50	37 (9.9%)
	51–60	31 (8.3%)
	61–70	12 (3.2%)
	71–80	5 (1.3%)
	Unknown	22 (5.9%)
Mode of inheritance	Autosomal dominant	92 (24.7%)
	Autosomal recessive	52 (13.9%)
	Maternal	47 (12.6%)
	X-linked	0
	Sporadic	179 (48.0%)
	Unknown	3 (0.8%)
Type of audiogram	High-frequency steeply sloping	80 (21.4%)
	High-frequency gently sloping	104 (27.9%)
	Flat	39 (10.5%)
	U-shaped (cookiebite)	39 (10.5%)
	Reverse U-shaped	4 (1.1%)
	Low frequency	39 (10.5%)
	Deafness	21 (5.6%)
	Others	43 (11.5%)
	Unknown	4 (1.1%)
	Total	373

Material and methods

Study population

The study population comprised 373 unrelated Japanese patients with suspected hereditary HL and 480 controls. The patients had visited the outpatient clinic of the Department of Otolaryngology, University Hospital of Medicine, Tokyo Medical and Dental University. Background characteristics of these patients are shown in Table I and were described previously [7]. These patients were suspected of having hereditary HL because they had a family history of it or because they had no other apparent cause of HL. We had previously detected the m.1555A>G and the m.3243A>G mutations in a total of 20 of these patients [7]. Because these mutations are located in mtDNA and thought to contribute strongly to the phenotypic expression of HL, we excluded these 20 patients from the case-control analysis. The average age of the remaining 353 patients was 40.9 ± 18.6 years, with an age range between 1 and 84 years; and the study group comprised 138 males and 215 females. As controls, 480 individuals with no manifestation of HL were selected from the National Institute of Health and Nutrition and were enrolled in this study. The control subjects comprised 143 males and 337 females. Their average age was 52.5 ± 12.3 years, with an age range between 23 and 85 years.

The study protocol complied with the Declaration of Helsinki. It was also approved by the Committee on the Ethics of Human Research of the Tokyo Metropolitan Institute of Gerontology, the Institutional Review Board (IRB no. 68) of Tokyo Medical and Dental University, and the Committee on the Ethics of Human Research of the National Institute of Health and Nutrition. This study was carried out only after obtaining the written informed consent from each individual and/or the parents in the case of children.

Selection of mitochondrial polymorphisms for haplogroup classification

By using our mtSNP database (http://mtsnp.tmig.or.jp/mtsnp/index.shtml) and phylogenetic tree of the Japanese [8], we selected 151 polymorphic sites that have been useful for classification of mitochondrial haplogroups. We selected a further 32 mtSNPs that define the 12 major haplogroups (i.e. F, B, A, N9a, N9b, M7a, M7b, G1, G2, D4a, D4b, and D5) found in Japan (Table II).

Genotyping of polymorphisms

The DNA samples were purified from the blood by using a standard procedure. In all, 186 genotypes of mtDNA polymorphisms were determined (G&G Science Corporation, Fukushima, Japan) by a method that combines the PCR and sequence-specific oligonucleotide probes with the use of suspension array technology (Luminex® 100™; Luminex, Austin, TX, USA) [9]. Details of the methodology used for genotyping, including the primers and probes for haplotyping, were given previously [10]. To confirm the accuracy of genotyping by this method, we subjected 91 DNA samples whose entire sequence